Phil. Trans. R. Soc. Lond. B **307**, 353–398 (1985) [353]
Printed in Great Britain

A MODEL OF CARDIAC ELECTRICAL ACTIVITY INCORPORATING IONIC PUMPS AND CONCENTRATION CHANGES

By D. DiFrancesco[1] and D. Noble, F.R.S.[2]

[1]*Dipartimento di Fisiologia e Biochimica Generali, Sez Elettrofisiologia, Via Celoria*, 26, 20133 *Milano, Italy*

[2]*University Laboratory of Physiology, Parks Road, Oxford, OX*1 3*PT, U.K.*

(*Received* 8 *February* 1984)

CONTENTS

Equations have been developed to describe cardiac action potentials and pacemaker activity. The model takes account of extensive developments in experimental work since the formulation of the M.N.T. (R. E. McAllister, D. Noble and R. W. Tsien, *J. Physiol., Lond.* **251**, 1–59 (1975)) and B.R. (G. W. Beeler and H. Reuter, *J. Physiol., Lond.* **268**, 177–210 (1977)) equations.

The current mechanism i_{K2} has been replaced by the hyperpolarizing-activated current, i_f. Depletion and accumulation of potassium ions in the extracellular space are represented either by partial differential equations for diffusion in cylindrical or spherical preparations or, when such accuracy is not essential, by a three-compartment model in which the extracellular concentration in the intercellular space is uniform. The description of the delayed K current, i_K, remains based on the work of D. Noble and R. W. Tsien (*J. Physiol., Lond.* **200**, 205–231 (1969*a*)). The instantaneous inward-rectifier, i_{K1}, is based on S. Hagiwara and K. Takahashi's equation (*J. Membrane Biol.* **18**, 61–80 (1974)) and on the patch clamp studies of B. Sakmann and G. Trube (*J. Physiol., Lond.* **347**, 641–658 (1984)) and of Y. Momose, G. Szabo and W. R. Giles (*Biophys. J.* **41**, 311a (1983)). The equations successfully account for all the properties formerly attributed to i_{K2}, as well as giving more complete descriptions of i_{K1} and i_K.

The sodium current equations are based on experimental data of T. J. Colatsky (*J. Physiol., Lond.* **305**, 215–234 (1980)) and A. M. Brown, K. S. Lee and T. Powell (*J. Physiol., Lond.* **318**, 479–500 (1981)). The equations correctly reproduce the range and magnitude of the sodium 'window' current.

The second inward current is based in part on the data of H. Reuter and H. Scholz (*J. Physiol., Lond.* **264**, 17–47 (1977)) and K. S. Lee and R. W. Tsien (*Nature, Lond.* **297**, 498–501 (1982)) so far as the ion selectivity is concerned. However, the activation and inactivation gating kinetics have been greatly speeded up to reproduce the very much faster currents recorded in recent work. A major consequence of this change is that Ca current inactivation mostly occurs very early in the action potential plateau.

The sodium–potassium exchange pump equations are based on data reported by D. C. Gadsby (*Proc. natn. Acad. Sci. U.S.A.* **77**, 4035–4039 (1980)) and by D. A. Eisner and W. J. Lederer (*J. Physiol., Lond.* **303**, 441–474 (1980)). The sodium–calcium exchange current is based on L. J. Mullins' equations (*J. gen. Physiol.* **70**, 681–695 (1977)). Intracellular calcium sequestration is represented by simple equations for uptake into a reticulum store which then reprimes a release store. The repriming equations use the data of W. R. Gibbons & H. A. Fozzard (*J. gen. Physiol.* **65**, 367–384 (1975*b*)). Following Fabiato & Fabiato's work (*J. Physiol., Lond.* **249**, 469–495 (1975)), Ca release is assumed to be triggered by intracellular free calcium. The equations reproduce the essential features of intracellular free calcium transients as measured with aequorin.

The explanatory range of the model entirely includes and greatly extends that of the M.N.T. equations. Despite the major changes made, the overall time-course of

the conductance changes to potassium ions strongly resembles that of the M.N.T. model. There are however important differences in the time courses of Na and Ca conductance changes. The Na conductance now includes a component due to the hyperpolarizing-activated current, i_f, which slowly increases during the pacemaker depolarization. The Ca conductance changes are very much faster than in the M.N.T. model so that in action potentials longer than about 50 ms the primary contribution of the fast gated calcium channel to the plateau is due to a steady-state 'window' current or non-inactivated component. Slower calcium or Ca-activated currents, such as the Na–Ca exchange current, or Ca-gated currents, or a much slower Ca channel must then play the dynamic role previously attributed to the kinetics of a single type of calcium channel. This feature of the model in turn means that the repolarization process should be related to the inotropic state, as indicated by experimental work.

The model successfully reproduces intracellular sodium concentration changes produced by variations in $[Na]_o$, or Na–K pump block. The sodium dependence of the overshoot potential is well reproduced despite the fact that steady state intracellular Na is proportional to extracellular Na, as in the experimental results of D. Ellis *J. Physiol., Lond.* **274**, 211–240 (1977)).

The model reproduces the responses to current pulses applied during the plateau and pacemaker phases. In particular, a substantial net decrease in conductance is predicted during the pacemaker depolarization despite the fact that the controlling process is an increase in conductance for the hyperpolarizing-activated current.

The immediate effects of changing extracellular [K] are reproduced, including: (i) the shortening of action potential duration and suppression of pacemaker activity at high [K]; (ii) the increased automaticity at moderately low [K]; and (iii) the depolarization to the plateau range with premature depolarizations and low voltage oscillations at very low [K].

The ionic currents attributed to changes in Na–K pump activity are well reproduced. It is shown that the apparent K_m for K activation of the pump depends strongly on the size of the restricted extracellular space. With a 30% space (as in canine Purkinje fibres) the apparent K_m is close to the assumed real value of 1 mM. When the extracellular space is reduced to below 5%, the apparent K_m increases by up to an order of magnitude. A substantial part of the pump is then not available for inhibition by low $[K]_b$. These results can explain the apparent discrepancies in the literature concerning the K_m for pump activation.

Definition of symbols

Voltages are in millivolts, concentrations in millimoles per litre, currents in nanoamperes.

t	time (seconds)
E_m	membrane potential
E_{Na}	sodium equilibrium potential
E_{Ca}	calcium equilibrium potential
E_K	potassium equilibrium potential
i_{tot}	total membrane ionic current flow
C	membrane capacitance (microfarads)
a	radius of preparation (micrometres)
l	length of preparation (micrometres)
x	radial distance (micrometres)
D	K^+ ion diffusion constant

V	total volume of preparation (microlitres)
V_i	total intracellular volume (microlitres)
V_e	total extracellular volume (microlitres)
V_{up}	volume of sarcoplasmic reticulum (s.r.) uptake store
V_{rel}	volume of store of releasable calcium (note: no assumptions are made on whether these stores are physically distinct)
V_{ecs}	fraction occupied by extracellular space
F	Faraday constant
$[Na]_o$, $[Na]_i$	extra- and intracellular Na concentrations (millimoles per litre)
$[K]_b$, $[K]_c$, $[K]_i$	bulk, cleft and intracellular K concentrations
$[Ca]_o$, $[Ca]_i$	extra- and intracellular Ca concentrations
$[Ca]_{up}$, $[Ca]_{rel}$	Ca concentrations in s.r. uptake and release stores
$[\overline{Ca}]_{up}$	maximum concentration in s.r. uptake store
$i_{b,Na}$	sodium background current
$g_{b,Na}$	sodium background conductance
i_p	sodium–potassium exchange pump current
$\bar{i}_p$	maximum value of i_p
$K_{m,K}$	K_m for K activation of Na–K pump
$K_{m,Na}$	K_m for Na activation of Na–K pump
i_{NaCa}	Na–Ca exchange current
k_{NaCa}	scaling factor for i_{NaCa}
E_{NaCa}	reversal potential for i_{NaCa}
n_{NaCa}	stoichiometry of Na–Ca exchange (Na:Ca)
γ_{NaCa}	position of energy barrier controlling voltage-dependence of i_{NaCa}
d_{NaCa}	denominator constant for i_{NaCa}
$i_{b,Ca}$	calcium background current
$g_{b,Ca}$	calcium background conductance
i_{Na}	TTX sensitive fast sodium current
g_{Na}	conductance of i_{Na} channels
m, α_m, β_m	activation gate and rate coefficients
h, α_h, β_h	inactivation gate and rate coefficients
E_{mh}	Reversal potential for sodium channel
i_{si}	total TTX-insensitive inward current (the 'second inward current')
$i_{Ca,f}$	fast calcium current (first component of i_{si})
$\bar{i}_{Ca,f}$	fully-activated value of $i_{Ca,f}$
$i_{Ca,s}$	slow calcium current (third component of i_{si})
$i_{si,Ca}$, $i_{si,Na}$, $i_{si,K}$	Ca, Na and K components of $i_{Ca,f}$
d, α_d, β_d	activation gating and rate coefficients for $i_{Ca,f}$
f, α_f, β_f	inactivation gating and rate coefficients for $i_{Ca,f}$
f_2, α_{f2}, β_{f2}	Ca_i dependent inactivation of $i_{Ca,f}$
$i_{m,Na}$, $i_{m,K}$, $i_{m,Ca}$	net membrane fluxes expressed as currents
E_{rev}	'reversal potential' for i_{K2}
$K_{m,Ca}$	K_m for Ca binding to release site
r	number of Ca ions required to bind to activate release
i_{up}	Ca uptake into s.r. expressed as a current

i_{tr}	Ca transferred into releasable form
i_{rel}	Ca release
p	variable controlling transfer of Ca to release sites
τ_{up}	time constant for s.r. uptake of calcium
τ_{rep}	time constant for repriming release store
τ_{rel}	time constant for Ca release (note: these time constants are not necessarily the overall time constants: see equations (42) to (51) for more details)
i_f	hyperpolarizing-activated Na–K current (nearest equivalent to i_{K2} in M.N.T. model)
$\bar{i}_f$	fully-activated value of i_f
$K_{m,f}$	K_m for extracellular K activation of i_f
$g_{f,K}$	K conductance of i_f channels
$g_{f,Na}$	Na conductance of i_f channels
y, α_y, β_y	gating variable and rate coefficients for i_f
i_K	delayed K current (equivalent of i_x in M.N.T. model)
$\bar{i}_K$	fully activated value of i_K
$i_{K,max}$	maximum outward current carried by i_K (at $[K]_i = 140$ mM)
x, α_x, β_x	gating variable and rate coefficients for i_K
i_{K1}	background K current (inward rectifier)
$K_{m,K1}$	K_m for K activation of i_{K1}
i_{to}	transient outward current
$K_{m,to}$	K_m for $[Ca]_i$ activation of i_{to}

Introduction

In 1975, McAllister *et al.* published a model of Purkinje fibre electrical activity. This model (which in the present paper we shall refer to as the M.N.T. model) represented the ionic currents using gating equations of the Hodgkin–Huxley form, and was based on Noble & Tsien's (1968, 1969*a*, *b*) experimental analysis of slow ionic current mechanisms together with Beeler & Reuter's (1970*a*, *b*) work on the second inward current. Beeler & Reuter (1977) subsequently developed a similar model for ventricular activity.

The very substantial delay between the experimental and theoretical papers reflects, in part, the difficulties involved. Detailed experimental information on some of the important currents (i_{Na} in particular) was scanty, and it was a matter for judgement to decide when a worthwhile model had been developed. That was bound to be a difficult judgement given the nature of the arguments on the use of voltage clamp techniques in the heart (Johnson & Lieberman 1971; Attwell & Cohen 1977; Beeler & McGuigan 1978).

However useful the M.N.T. model may have been, it has now outlived that usefulness, and for a variety of reasons. First, one of the major elements of the model, that is, the i_{K2} system, has recently been radically re-interpreted (DiFrancesco 1981*a*, *b*; DiFrancesco & Noble 1980*a*, 1981, 1982). Secondly, much better experimental information on the sodium current in the heart (Lee *et al.* 1979; Ebihara *et al.* 1980; Brown *et al.* 1981) and in Purkinje fibres in particular (Colatsky 1980) is now available. Thirdly, it has become increasingly important to take account of intracellular and extracellular ion concentration changes and, therefore, of the influence of ionic pumps, exchange mechanisms and of restricted diffusion. Good experimental information is also now available on the sodium pump in Purkinje fibres (Isenberg & Trautwein 1974; Ellis 1977; Deitmer & Ellis 1978; Gadsby 1980; Eisner & Lederer 1980) and on the influence of extracellular potassium ions on potassium and potassium-dependent currents (DiFrancesco & McNaughton 1979; DiFrancesco *et al.* 1979*b*; Brown *et al.* 1980).

Some information is also available on the sodium–calcium exchange process (Horackova & Vassort 1979; Chapman & Tunstall 1980; Coraboeuf *et al.* 1981; Fischmeister & Vassort 1981; Sheu & Fozzard 1982; Mentrard & Vassort 1982), and the possible equations for an electrogenic Na–Ca exchange have recently been reviewed by Mullins (1977, 1981). We have incorporated this information together with modelling of the Ca sequestration and release mechanisms based on the data given by Chapman (1979) and on the calcium-induced calcium release hypothesis of Fabiato & Fabiato (1975). Important changes have also occurred in the description and analysis of the second inward current (see review by Noble 1984).

Initially, our work was directed towards the question whether all the properties of 'i_{K2}' and of the pacemaker potential that had led, apparently so conclusively, to the i_{K2} hypothesis were compatible with the new interpretation of this mechanism as an inward, largely sodium, current i_f that is activated by hyperpolarization. The answer to that question is that these properties, including the 'Nernstian' behaviour of the reversal potential (E_{K2}) (DiFrancesco & Noble 1980*a*), inward-going rectification, the 'cross-over' phenomenon, and the slope conductance changes are indeed fully compatible with the new interpretation, and that some other properties, such as the disappearance of 'i_{K2}' in sodium-free solutions (McAllister & Noble 1966; DiFrancesco & Noble 1980*b*) and the otherwise anomalous conductance measurements reported by DiFrancesco (1981*a*), now receive natural explanations that were not within the scope of the i_{K2} hypothesis or the M.N.T. model. A full account of this work has recently appeared in the Amsterdam symposium on cardiac rate and rhythm (DiFrancesco & Noble 1982). In the present paper we shall refer only fairly briefly to the relevant results presented in that paper using an earlier and much simpler version of the equations.

The work for the Amsterdam paper was limited to answering a particular and pressing question, but it clearly formed the basis for the more ambitious undertaking to develop a model that incorporates the full explanatory range of the M.N.T. equations and the greatly extended range that is now possible with the newer results referred to above. It is this development that we report in this paper and in a subsequent paper (DiFrancesco *et al.* 1985). Accompanying papers (Noble & Noble 1984; Brown *et al.* 1984*a*, *b*) describe the extension of the model to the mammalian s.a. node and its application to experimental results in that tissue.

Description of equations

We have chosen to use absolute units of current (in nanoamperes) scaled to give currents similar to those recorded experimentally in a Purkinje strand of length 2 mm and radius 50 μm. The reason for choosing this convention rather than using current density is that in many of the calculations current density varies as a function of position in the preparation (to take account of concentration profiles in the extracellular space). With regard to K-dependent currents therefore a single current density might be a misleading parameter. The magnitudes were sometimes scaled up or down to give currents for larger or smaller preparations. The surface area of our standard fibre is 0.0063 cm^2. Assuming that the total cell membrane area is ten times larger than the cylinder surface (Mobley & Page 1972), the total cell surface would be 0.063 cm². Thus, to convert our figures to nanoamperes per square centimetre the currents should be multiplied by a factor of about 15. We have assumed a membrane capacitance of 12 μF cm^{-2} of cylinder surface (Weidmann 1952) or 1.2 μF cm^{-2} of cell surface, which gives a value of 0.0756 μF for our standard preparation.

The differential equation for the variation of membrane potential, E_m, is

$$\mathrm{d}E_m/\mathrm{d}t = -i_{tot}/C \tag{1}$$

where C is the membrane capacitance and i_{tot} is the total current:

$$i_{tot} = i_f + i_K + i_{K1} + i_{to} + i_{b,\,Na} + i_{b,\,Ca} + i_p + i_{NaCa} + i_{Na} + i_{Ca,\,f} + i_{Ca,\,s} + i_{pulse}. \tag{2}$$

Each of these current components will now be explained in turn.

(a) *Hyperpolarizing-activated current*, i_f

The experimental evidence (DiFrancesco 1981*a*) shows that the fully activated current–voltage relation for this channel is nearly linear. Some of the deviation from linearity, particularly at extreme negative potentials, might be attributed to residual K ion depletion in the extracellular space, although the presence of outward-going rectification at high K^+ concentrations (DiFrancesco 1982) argues in favour of it being in part a genuine channel property. Nevertheless, a linear i_f function is a good approximation in the pacemaker range of potentials where i_f has its most important functional role. The behaviour of the reversal potential is consistent with the view that the total current is composed of relatively independent Na^+ and K^+ components and that, at normal K^+ and Na^+ concentrations, the contributions of these two ions to the total conductance are approximately equal. The net reversal potential in normal physiological solutions is then around −20 mV. At high values of external bulk potassium $[K]_b$, the current is greatly increased (DiFrancesco 1981*b*). This property suggests that the channel is activated by external potassium. We have assumed a simple first-order binding process for this activation. The experimental value for $K_{m,\,f}$ (that is, the value of $[K]_b$ for half activation) is 45 mM (DiFrancesco 1982). In Na-free solutions, only the K^+ component is present. This then shows a reversal potential close to the expected value for E_K (Hart *et al.* 1980).

The equation we shall use for the fully activated current, i_f, is therefore:

$$i_f = ([K]_c/([K]_c + K_{m,\,f}))\,\{g_{f,\,K}(E-E_K) + g_{f,\,Na}(E-E_{Na})\}. \tag{3}$$

Suitable experimental values for the constants in this equation are $g_{f,\,Na} = 3$ μS, $g_{f,\,K} = 3$ μS, $K_{m,\,f} = 45$ mM (DiFrancesco 1981*b*, 1982).

The gating mechanism controlling i_f is the s process described by Noble & Tsien (1968), except that activation occurs on hyperpolarization, not depolarization. The fully activated state in our model therefore corresponds to the fully deactivated state in Noble & Tsien's analysis. We have chosen the variable y to represent the degree of activation of i_f. So, $y = 1 - s$. The equations for α_y and β_y are those in the M.N.T. model for β_s and α_s respectively:

$$\mathrm{d}y/\mathrm{d}t = \alpha_y(1-y) - \beta_y\,y \tag{4}$$

where:

$$\alpha_y = 0.025\exp(-0.067(E+52)), \tag{5}$$

$$\beta_y = 0.5\,(E+52)/(1-\exp(0.2(E+52))), \tag{6}$$

$$(\beta_y)_{E=-52} = 2.5. \tag{6a}$$

The net current is then given by:

$$i_f = y\bar{i}_f. \tag{7}$$

It should be noted that, while these equations assume first-order voltage-dependent kinetics for the gating parameter, y, the most recent experimental data (DiFrancesco & Ferroni 1983; Hart 1983; DiFrancesco 1984) shows that the onset of i_f is in fact sigmoid: there is a delay in the time course which can be removed by conditioning hyperpolarizations. This property, which is of course important for detailed modelling of channel properties, does not have much importance in reconstructing the pacemaker potential since in the relevant voltage range the current is very slow and an initial small delay not too important. For simplicity we have retained the M.N.T. first-order kinetics, though these could readily be substituted in the program by more complex equations without significant change in the results computed here.

(b) *Time-dependent (delayed)* K^+ *current*, i_K

A considerable amount of new experimental information has appeared on this current since the M.N.T. equations were formulated. First, it has been shown in a variety of preparations (Purkinje fibres: DiFrancesco & McNaughton 1979; frog atrium: Brown *et al.* 1980; ventricle: McDonald & Trautwein 1978; Rabbit s.a. node: DiFrancesco *et al.* 1979) that, while the instantaneous current–voltage relation shows inward-going rectification without a negative slope conductance region (as first shown by Noble & Tsien 1969*a*), it does *not* show the cross-over phenomenon, that is, at all potentials, the current is a monotonic function of $[K]_c$. In this respect, the current differs quite markedly from i_{K1}. The absence of the cross-over effect allows us to use a very simple formulation both for the rectification property and for the K^+ dependence of the current. This is based on using rate theory, assuming that the major energy barrier for ion movement in the electric field is situated at the inner surface of the membrane (Noble 1972; Jack *et al.* 1975). This gives the equation:

$$i_K = i_{K,\max}\{[K]_i - [K]_c \exp(-E/25)\}/140. \tag{8}$$

The usual value used for the 'maximum' current (actually the maximum outward current at positive potentials when $[K]_i = 140$ mM) is 180 nA. $[K]_i$ was usually set to 140 mM (Lee & Fozzard 1975; Miura *et al.* 1977). These parameters give outward currents similar to the delayed outward current recorded by Noble & Tsien (1969*a*).

Notice that, following McDonald & Trautwein (1978), we have chosen the symbol i_K for this current rather than the symbol i_x used by Noble & Tsien (1969*a*). The justification for this change is that, in the M.N.T. model, E_{K2} is regarded as the true value of E_K. Since this was considerably *negative* to the reversal potential for the delayed current activated in the plateau range of potentials, it was concluded that the latter was a less specific channel. The new interpretation of E_{K2} as a mixed 'reversal' potential means that the true value of E_K is almost certainly 10–20 mV positive to E_{K2} (see DiFrancesco & Noble (1982) for an equation relating E_{K2} to the true value of E_K), so that the reversal potential for the plateau-activated current is much closer to E_K than in the M.N.T. equations. We have therefore regarded it as a specific K^+ current for which it is more natural to use the symbol i_K. While this current should clearly *not* be confused with i_{K2} in the M.N.T. model, it *does* correspond to the g_{K2} system first described by Hall *et al.* (1973) which was used in the 1962 model (Nobel 1962). In several respects, our formulation of the equations for K^+ currents closely resembles the 1962 model and its development (Noble 1965) to account for extracellular K^+ effects.

The second aspect of this system that has been investigated further experimentally is the fact, also first observed by Noble & Tsien (1969*a*), that at least two and sometimes three exponential terms are required fully to describe the time course of the current following voltage step changes. This feature has been confirmed in all the multicellular preparations investigated so far with a wide variety of different voltage clamp techniques, though the detailed kinetics sometimes differ from those of Noble & Tsien (see, for example, Brown *et al.* 1972) even in Purkinje fibres (R. H. Brown and D. Noble, unpublished). The question that arises is whether this reflects a genuine property of the gating process or whether it is produced partly or even wholly by perturbations due to ion concentration changes. The most complete analysis of this problem (Brown *et al.* 1980; DiFrancesco & Noble 1980*a*) shows that the slowest exponential term, when present, is indeed due to a K^+ accumulation process but that, although this necessarily perturbs the time course of i_K (Attwell *et al.* 1979*b*), this perturbation does not account for the biexponential time course of the remaining components, whose time constants are not seriously perturbed. We are therefore left with the problem faced by Noble & Tsien (1969*a*) that a single Hodgkin–Huxley type gating reaction does not account for the current time course. We will adopt the same solution as Noble & Tsien (1969*a*) that is, to note, like them, that only one of the components is of significant importance during repolarization (Noble & Tsien 1969*b*). For simplicity, we shall drop subscripts and use the gating symbol x for the controlling reaction:

$$\mathrm{d}x/\mathrm{d}t = \alpha_x(1-x)-\beta_x x, \tag{9}$$

$$\alpha_x = 0.5 \exp\,(0.0826\,(E+50))/(1+\exp\,(0.057\,(E+50))), \tag{10}$$

$$\beta_x = 1.3 \exp\,(-0.06\,(E+20))/(1+\exp\,(-0.04\,(E+20))) \tag{11}$$

where the equations for α_x and β_x are those used in the M.N.T. model. The total current is given by

$$i_K = x\bar{i}_K. \tag{12}$$

(*c*) *Time-independent* (*background*) K^+ *current*, i_{K1}

The M.N.T. model represented this current by a purely empirical function describing inward-going rectification with a negative slope over a range of potentials positive to the resting potential. Since this current is obtained by measuring the current that remains when other identifiable components have been subtracted (in this respect it is exactly analogous to the leak current in the original Hodgkin–Huxley (1952) analysis), it has always been evident that it must include currents other than the true i_{K1}, such as the pump and exchange currents. In the new model we represent these currents by separate equations (see below). This is one reason why our i_{K1} cannot correspond exactly to that in the M.N.T. model. Furthermore, since the state $y = 0$ in our model corresponds to the state $s = 1$ in the M.N.T. model, a term corresponding to i_{K2} in that model now becomes indistinguishable from i_{K1} (for a further explanation of the mapping between these aspects of the two models see DiFrancesco & Noble (1982)).

These changes simply add or subtract to the magnitude and slightly change the form of i_{K1}. A more radical question is whether the basic form of the i_{K1} function is correct or whether it is possible that features such as inward-going rectification are not properties of a single mechanism, but reflect rather our ignorance of some unidentified component. This question acquires added force since we have ourselves shown that the 'inward-going rectification displayed by i_{K2} is not a genuine property of a single mechanism (DiFrancesco & Noble 1982, figure 4).

The most direct way of answering this question is to measure K^+ fluxes as a function of potential. This was first done by Haas & Kern (1966) who showed that the radioactive flux was consistent with the presence of inward-going rectification. Recently, Vereecke *et al.* (1980) have used a much improved technique to show not only that the K^+ efflux is consistent with the presence of inward-going rectification but also that the negative slope region is a genuine characteristic. Clear-cut evidence of the inward-rectifying property comes also from experiments where the i_{K1} (E) relation is measured by substracting the time-independent curves in the presence and absence of Ba^{2+} ions (DiFrancesco 1981 *b*). Finally, recent work with patch-clamp techniques (Momose *et al.* 1983; Sakmann & Trube 1984) shows the presence of i_{K1} and has provided valuable data on its kinetics and $[K]_o$-activation at potentials negative to E_K.

In place of the purely empirical formulation of the M.N.T. model we have chosen to use Hagiwara & Takahashi's (1974) equation. This is also empirical but it is a simple formulation which closely resembles the curves generated by the more complex equations for the blocking particle model of Hille & Schwarz (1978; see their comparison in figure 9 of that paper). We have also incorporated the fact that the channel is K^+ activated (cf. the development of the M.N.T. equations by Cohen *et al.* (1978) and the patch clamp data of Sakmann & Trube (1984)). Our equation is:

$$i_{K1} = g_{K1}([K]_c/([K]_c+K_{m,1}))\,\{(E-E_K)/(1+\exp\,((E-E_K+10)\;2F/RT))\}. \qquad (13)$$

$K_{m,1}$ was set to 210 mM (Sakmann & Trube 1984, figure 5) and the maximum conductance (which is the maximum conductance reached during strong hyperpolarizations) was set to 920 μS. We shall show later that this reproduces the main experimental features of the current–voltage relations attributable to i_{K1}.

Carmeliet (1982) has recently raised the question whether i_{K1} is strictly instantaneous. The patch-clamp work indeed shows that there is time-dependent inactivation (Sakmann & Trube 1984) but since this time-dependence becomes important only at very negative potentials we have not used equations for this process. If needed, they could easily be incorporated into the program.

(*d*) *The transient outward current*, i_{to}

It has been known since the first studies of i_{K1} that, beyond about -20 mV, the inward rectifier is either masked by a rapidly activated outward rectifier or that the i_{K1} channel itself shows outward rectification positive to -20 mV. The experimental evidence (including the action of blocking agents like Ba^{2+} and Cs^{2+} on inward but not outward-going rectification) favours the first interpretation (see Isenberg 1976; Carmeliet 1980) which is why our equation for i_{K1}, unlike that in the M.N.T. model, describes inward-going rectification only.

Flux measurements by Vereecke *et al.* (1980) favour the view that the outward-rectification, instantaneous and transient, is also largely carried by K^+ ions. The current is very sensitive to external K^+ ions (Hart *et al.* 1982), and is largely, but not entirely, blocked by 4-aminopyridine (Boyett 1981 *b*; Coraboeuf & Carmeliet 1982).

Originally, a Hodgkin–Huxley type model was used for this current which was attributed to Cl^- ions (see Dudel *et al.* 1967 *a*; Fozzard & Hiraoka 1973; McAllister *et al.* 1975). There are, however, serious difficulties with this interpretation. The time constants are in fact relatively independent of voltage and 'envelope' tests (cf. Noble & Tsien 1968) do not work (Hart *et al.* 1982). Moreover, Siegelbaum & Tsien (1980) have shown that the activation is $[Ca]_i$-dependent.

We have therefore represented i_{to} as an outward rectifier that is $[Ca]_i$-activated and which depends on $[K]_o$. As McAllister, Noble & Tsien (1975) have shown, the precise inactivation process for i_{to} is not important during a single action potential, though repriming of the process is important during repetitive firing (for example, Hauswirth *et al.* 1972; Boyett 1981*a*; Boyett & Jewell 1980). Moreover, the inactivation process is not well understood.

Our equation for the K^+ activation, Ca^{2+} activation and rectification properties of i_{to} is

$$\begin{aligned} i_{to} = {} & 0.28((0.2+[K]_c)/(K_{m,1}+[K]_c))\,([Ca]_i/(K_{m,to}+[Ca]_i)) \\ & \times\{(E+10)/(1-\exp(-0.2\,(E+10))\}\{([K]_i \exp(0.02\,E)-[K]_o\exp(-0.02\,E)\}. \end{aligned} \tag{14}$$

The first term in this equation represents activation by external $[K^+]$ which saturates at about 30 mM (Hart *et al.* 1982). The second term represents $[Ca]_i$ activation. We usually set $K_{m,to}$ to 1 μM, which allows the normal $[Ca]_i$ transient to activate the current with the correct magnitude and speed to reproduce Siegelbaum & Tsien's (1980) experimental results. The third term represents the voltage dependence (this term could be replaced by a gating process if desired). This term was set to 5 at $E = -10$. The final term is obtained from rate theory assuming that the energy barrier is placed at the centre of the membrane, which generates a moderate degree of outward rectification.

The inactivation process was described by a first order equation fitted to Fozzard & Hiraoka's (1973) data:

$$\alpha_r = 0.033 \exp(-E/17) \tag{15}$$

$$\beta_r = 33/(1+\exp(-(E+10)/8)) \tag{16}$$

$$\mathrm{d}r/\mathrm{d}t = \alpha_r(1-r)-\beta_r r \tag{17}$$

$$i_{to} = r\bar{i}_{to}. \tag{18}$$

(It should be noted that these equations represent the main features of i_{to} but they do not fully represent the multicomponent nature of i_{to}. This will be dealt with by DiFrancesco *et al.* (1985).)

(*e*) *Background sodium current*, $i_{b,Na}$

As in the M.N.T. model, the resting sodium flux is represented by a linear relation:

$$i_{b,Na} = g_{b,Na}(E-E_{Na}). \tag{19}$$

Setting $g_{b,Na}$ equal to 0.18 μS gives a resting sodium influx that is both sufficient to account for the deviation of E from E_K and for the rate of increase in intracellular sodium when the sodium pump is blocked (Ellis 1977).

When varying $[Na]_o$ in the computations, we have assumed that the fraction of $g_{b,Na}$ that is carried by sodium is proportional to $[Na]_o$. In effect, this assumption allows for the fact that common Na^+ substitutes like choline are known to permeate the membrane. The assumption of a linear dependence of the Na current on $[Na]_o$ is the simplest we could make but it turns out to be adequate for the present purposes. Equation (19) then becomes:

$$i_b = ([Na]_o/[Na]_{o,c})\,g_{b,Na}(E-E_{Na})+i_{b,Ch} \tag{20}$$

where $[Na]_{o,c}$ is the control level of $[Na]_o$ (usually 140 mM) and $i_{b,Ch}$ is the background current due to choline or another Na substitute. This equation assumes that Na and other ions move independently through the background channel. A further test of the value chosen for $g_{b,Na}$

is whether it allows accurate prediction of the rate of change of internal sodium following external sodium concentration changes. This is the case (see figure 9).

During the development of this model, Colquhoun *et al.* (1981) published patch-clamp studies of a linear non-specific cation channel activated by Ca^{2+} ions. It was initially tempting to conclude that this channel might account for the resting background conductance. This possibility was incorporated into the computer program by allowing an option to use a background conductance equally permeable to Na^+ and K^+ ions and which is Ca^{2+} activated. There are, however, serious difficulties in using this option (see Conclusions) and we have not used it in the present paper.

(*f*) Na–K *exchange pump current*, i_p

The Na–K exchange pump in Purkinje fibres has been extensively studied recently (Ellis 1977; Deitmer & Ellis 1978; Gadsby 1980; Gadsby & Cranefield 1979; Eisner & Lederer 1980; Eisner *et al.* 1981). The results agree in showing that the pump is directly electrogenic with a probable stoichiometry of 3:2 (Na:K). At rest, therefore, there must be an outward pump current, i_p, equal to one third of the net sodium influx generated by Na conducting channels and by the Na–Ca exchange process (see (*g*) below).

For simplicity, we have assumed that the pump is activated by external K^+ and by internal Na^+ by first-order binding processes:

$$i_p = \bar{i}_p([K]_c/(K_{m,K}+[K]_c))([Na]_i/(K_{m,Na}+[Na]_i)). \tag{21}$$

where $\bar{i}_p$ is the maximum pump current, $K_{m,K}$ is the value of $[K]_c$ for half-activation and $K_{m,Na}$ is the value of $[Na]_i$ for half-activation. The experimental evidence (Eisner *et al.* 1981) shows that over the whole range of values so far explored (up to about 20 mM) the pump rate is linearly dependent on $[Na]_i$. This means that $K_{m,Na}$ must be considerably larger than 20 mM. We have chosen to use 40 mM.

At first sight, there is considerable disagreement on the value of $K_{m,K}$. Gadsby (1980) obtained 1 mM in canine Purkinje fibres, whereas Eisner & Lederer (1980) obtained 4–5 mM in the sheep. Deitmer & Ellis (1978) obtained an even higher value (around 10 mM). We shall show in this paper that this variation is in fact compatible with a single value of $K_{m,K}$ provided that effects due to the restricted extracellular space are taken into account. On this view, the best value for $K_{m,K}$ is the lowest one obtained in the species with the largest extracellular space. We shall therefore use 1 mM for this parameter. This does in fact correspond well with the values in other tissues. With these values for the activation parameters, a maximum current of 125 nA gives a resting pump current of about 20 nA when $[K]_c = 4$ mM and $[Na]_i = 9$ mM. This current is similar to that estimated by extrapolating the $i_p([Na]_i)$ function of Eisner *et al.* (1981).

(*g*) Na–Ca *exchange current*, i_{NaCa}

The evidence that this exchange mechanism is directly electrogenic has recently been reviewed by Mullins (1981) who has also proposed that the current generated, which we will call i_{NaCa}, may replace some of the currents already identified in cardiac electrophysiology. We will discuss elsewhere the extent to which our results support this suggestion (see DiFrancesco *et al.* 1985 and also Brown *et al.* 1984*a*, *b*). Fischmeister & Vassort (1981) have recently incorporated the Na–Ca exchange current into the M.N.T. model (for a comparison, see DiFrancesco *et al.* 1985).

The equations for i_{NaCa} are based on the assumption that the only energy available to the process is that of the Na and Ca ion gradients and the membrane potential. Two alternative expressions have been used in our work. The simplest assumes that the current is a hyperbolic sine function of the energy gradient expressed in millivolts:

$$i_{NaCa} = k_{NaCa}\,\{\exp\,((E-E_{NaCa})\,F/RT) - \exp\,((-(E-E_{NaCa})F/RT\}/2 \tag{22}$$

where

$$E_{NaCa} = (n_{NaCa}E_{Na} - 2E_{Ca})/(n_{NaCa}-2), \tag{23}$$

$$E_{Na} = (RT/F)\,\ln\,([Na]_o/[Na]_i), \tag{24}$$

$$E_{Ca} = (RT/2F)\,\ln\,([Ca]_o/[Ca]_i) \tag{25}$$

and n_{NaCa} is the stoichiometry of the exchange. We have used either 3:1, as suggested by some of the experimental literature in the heart, or 4:1 as suggested by work on squid nerve (Mullins (1981) figure 4.3). Most of the results in this paper use 3:1 and the question whether 4:1 would equally well fit the results will be treated by DiFrancesco *et al.* (1985).

Equation (22) is given by Mullins (1977, 1981) as a simplification for his more general model. It may apply moderately well for sudden small voltage changes at fixed ion concentrations. There is however no reason to suppose that it will be at all accurate when large ion concentration changes are involved. In fact, the variations in $[Ca]_i$ may be one or two orders of magnitude during normal electrical activity and it is then important to use a more realistic function that reproduces the expected $[Ca]_i$ dependence of the exchange process. The full equations for the Mullins model are however very complex and many of the rate coefficients are unknown. We have therefore used an intermediate version based on the fact that sodium concentration changes are fairly small, at least during a few action potentials. Some of the terms in Mullins full equations are then constant and we obtain (26):

$$\begin{aligned} i_{NaCa} = k_{NaCa}\,(&\exp\,(\gamma(n_{NaCa}-2)\,EF/(2RT))[Na]_i{}^n[Ca]_o \\ &-\exp\,(-(1-\gamma)(n_{NaCa}-2)\,EF/(2RT))[Na]_o{}^n[Ca]_i)/ \\ &(1+d_{NaCa}([Ca]_i[Na]_o{}^n+[Ca]_o[Na]_i{}^n.) \end{aligned} \tag{26}$$

This equation would require further refinement (replacing 1 in the denominator by a function of the sodium concentrations) to take proper account of $[Na]_i$ and $[Na]_o$ changes. The variable γ was set to 0.5 in the standard model. This parameter represents the shape or position of the energy barrier in the electrical field and is exactly analogous to similar parameters used in rate theory to describe current–voltage relations (see, for example, Noble 1972). Some of the computations were run with values of γ set to the extreme values of 0 or 1. It was found that this produces some quantitative changes in the precise time course of i_{NaCa} during an action potential, but does not seriously change the qualitative aspects of the results.

Some of the variables in these equations are either fixed (for example, $[Na]_o$ is usually 140 mM, $[Ca]_o$ is usually 2 mM), or can be computed from the model (for example, $[Na]_i$ and $[Ca]_i$), or can be determined once other model parameters are fixed). Thus, k_{NaCa}, which scales the exchange current for a given energy gradient, can be determined as the value required to ensure that, in the steady state, all the calcium entering the cells is eventually pumped out. A suitable value for k_{NaCa} when $[Na]_i$ is in the range 5–10 mM and $[Ca]_i$ is in the range 0.05–0.1 μM is 20, when (22) is used. For (26) appropriate values are $k_{NaCa} = 0.02$ and $d_{NaCa} = 0.001$.

Finally, to keep the resting calcium in this range (as suggested by experimental results with aequorin and Ca electrodes – see Marban *et al.* 1980; Sheu & Fozzard 1982), we require a resting Ca^{2+} leak (cf. Fischmeister & Vassort 1981):

$$i_{b,\,Ca} = g_{b,\,Ca}\,(E - E_{Ca}). \tag{27}$$

A value of $g_{b,\,Ca}$ that satisfies the above conditions is 0.02 μS.

(*h*) *The fast sodium current*, i_{Na}

Major experimental advances have been made recently in measuring this current, the most important being the use small synthetic ventricular strands (Ebihara *et al.* 1980), rabbit Purkinje fibres (Colatsky & Tsien 1979; Colatsky 1980) and of single ventricular cells (Brown *et al.* 1981). These studies have provided more reliable information on the kinetics which are significantly different from those used in the M.N.T. model. Another approach has been to measure the steady-state properties by determining the TTX-sensitive steady state ('window') current (Attwell *et al.* 1979*a*).

The data that is most relevant for our purposes is that obtained on Purkinje fibres by Colatsky (1980). The major disadvantage of this data is that it was obtained in cooled fibres, which means that the speeds of the gating reactions must be adjusted to 37 °C. It is also possible that the inactivation curve shifts in a negative direction on the voltage axis at low temperature, which would reduce the overlap of the activation and inactivation curves. The single cell data at 37 °C does indeed show more overlap. Colatsky (1980) even concluded that there was no overlap in his experiments. We shall show that this is too strong a conclusion. Even with his data, we can reconstruct fairly easily the observed 'window' current (see below).

The equations we have used are:

$$i_{Na} = m^3h\,\{g_{Na}\,(E - E_{mh})\}, \tag{28}$$

$$E_{mh} = (RT/F)\,\ln\,(([Na]_o + 0.12\,[K]_c)/([Na]_i + 0.12\,[K]_i)) \tag{29}$$

that is, the sodium channel is assumed to show a 12% permeability to K^+ ions (Chandler & Meves 1965)

$$dm/dt = \alpha_m\,(1-m) - \beta_m\,m, \tag{30}$$

$$dh/dt = \alpha_h\,(1-h) - \beta_h\,h, \tag{31}$$

$$\alpha_m = 200(E+41)/(1-\exp\,(0.1\,(E+41)), \tag{32}$$

$$\alpha_{(m)E=-41} = 2000, \tag{33}$$

$$\beta_m = 8000\,\exp\,(-0.056(E+66)), \tag{34}$$

$$\alpha_h = 20\,\exp\,(-0.125\,(E+75)), \tag{35}$$

$$\beta_h = 2000/\{320\,\exp\,(-0.1(E+75))\}. \tag{36}$$

The value we have used for g_{Na} is 750 μS. This generates a maximum depolarization rate similar to that recorded experimentally. The maximum inward current on depolarizing to 0 mV is then about 3000 nA which, using the scaling factor of 15 for conversion to current density (see above) gives about 500 μA cm^{-2}, that is, the value recorded experimentally (Colatsky 1980).

The *m* equations used here are in fact that of Hodgkin & Huxley (1952) shifted on the voltage axis to give a steady state value of 0.5 for m^3 at -30 mV, which fits Colatsky's data – see below. The rate constants were then scaled to give a time constant, τ_m, of about 100 μs at $E = 0$ mV (Brown *et al.* 1981). It can be seen (see figure 4) that this gives an activation curve that is somewhat less steep than that obtained in Colatsky's experiments. Our reason for choosing a less steep function is that this fits better the experimental data of Brown *et al.* (1981) which was obtained in more favourable conditions. The greater steepness of Colatsky's curve could be due to a small degree of voltage non-uniformity in a multicellular preparation which would be minimized in a single cell clamp.

The h equations were fitted to Colatsky's data to give $h_\infty = 0.5$ at $E = -70$ mV. This in fact corresponds well to one of Colatsky's published curves but it is worth noting that his half-inactivation potential is usually nearer -75 mV, which may well be due to cooling the fibres. The absolute values for the rate constants were adjusted to give τ_h values of about 50 ms at -80 mV, decreasing to 0.7 ms at 0 mV. Brown *et al.* (1981) also found a steep voltage dependence for τ_h between the resting potential, where τ_h is very large, and 0 mV, where it becomes very small. This means that, during a normal action potential, the inactivation is considerably faster than in the M.N.T. model.

These equations do not reproduce slower components of Na inactivation and recovery. Gintant *et al.* (1984) and E. Carmeliet (personal communication) have very recently shown that such a process does exist and that the 'window' current is considerably larger at the beginning of the plateau than at its end, that is, a small but significant component of Na current inactivates with a time course of several hundred milliseconds. In this connection it is worth noting that a persistent problem in our computations has been the presence (though not in the particular computations illustrated in this paper) of a small bump on the repolarization process which is due to the 'window' current. Introducing slow inactivation would be one way of eliminating this problem.

(*i*) *The second inward current, i_{si}, and its components*

Considerable advances have been made in studying this current since the formulation of the M.N.T. and B.R. equations.

First, Reuter & Scholz (1977) showed that the reversal potential for i_{si} requires that some K^+ ions should cross the channel in addition to Ca^{2+} ions. This view, has been confirmed in the work of Lee & Tsien (1982) using a perfusion electrode clamp of single guinea-pig ventricular cells. Reuter & Scholz also concluded that Na^+ ions cross the channel. This conclusion is now doubtful (see Mitchell *et al.* 1983; Noble 1984). Our computer program allows for this possibility but we have not used this facility in most of our computations.

Second, the work with isolated cells shows that the kinetics of the largest component of i_{si} are *very much* faster than in the M.N.T. and B.R. models. Activation peaks occur within 2–3 ms and the inactivation time constant lies in the range 10–20 ms (see review by Noble 1984). These figures are at least an order of magnitude faster than previously supposed.

Third, the peak amplitude of the calcium current is considerably greater than the multicellular work suggested (see discussion in Mitchell *et al.* 1983).

Finally, there is evidence for two or three different components of i_{si}. In addition to the fast component, which we will call $i_{Ca,f}$, a Cd^{2+} and Mn^{2+} resistant channel has been found in single guinea-pig ventricular cells (Lee *et al.* 1984*a*) and in single frog atrial cells (Hume & Giles 1983). This component is very slowly and, at some voltages, only partly inactivated.

In some ways, therefore, it may play a role similar to the non-inactivated component of i_{si} in the M.N.T. equations for which experimental evidence was recently presented by Kass & Wiegers (1982).

However, there is also another component that may play this role. This is strongly correlated with contraction and may, therefore, be $[Ca]_i$-activated. It has been found and called $i_{si,2}$ in the mammalian s.a. node (Brown *et al.* 1983, 1984*a*) and in single guinea-pig ventricular cells (Lee *et al.* 1983, 1984*b*). One interpretation of this is that it is carried by the Na–Ca exchange process for which we have given equations in a previous section. One of the purposes of our model is to explore the extent to which these equations reproduce the properties of $i_{si,2}$ in Purkinje fibres, the s.a. node and in single ventricular cells.

For the fast component, $i_{Ca,f}$, we have followed Reuter & Scholz (1977) in using a constant field type formulation for the individual ion movements (though see Attwell & Jack 1978) for an important critique of this approach).

$$i_{Ca,f} = dff2\,(i_{si,Ca} + i_{si,K}), \tag{37}$$

$$i_{si,Ca} = 4\,P_{si}\,(E-50)\;(F^2/RT)/(1-\exp\,(-(E-50)\;2F/RT))$$
$$\times \{[Ca]_i \exp\,(100F/RT) - [Ca]_o \exp\,(-2(E-50)\;F/RT)\}, \tag{38}$$

$$i_{si,K} = 0.01\;P_{si}\,(E-50)\;(F^2/RT)/(1-\exp\,(-(E-50)\,F/RT))$$
$$\times \{[K]_i \exp\,(50F/RT) - [K]_c \exp\,(-(E-50)\,F/RT)\}. \tag{39}$$

If required, an equation similar to (39) was used for describing a sodium component.

Note that, in these equations, we do not use an explicit equation for the reversal potential. When required (for example, for calculations of conductance), this was computed either by an iterative procedure or by solving the quadratic equation given by Attwell & Jack (1978).

We now require a description of the gating kinetics (d and f). The original Beeler & Reuter (1977) equations used in the M.N.T. model describe an activation gate, d, with a time constant of about 22 ms at about 0 mV and an inactivation gate with a very long time constant (about 300 ms). This was a very important feature of the M.N.T. and Beeler–Reuter models since the process of i_{si} inactivation is then strongly implicated in controlling the duration of the action potential plateau. More recent work shows that both activation and inactivation occur very much more quickly than in the M.N.T. model. In Purkinje fibres, the most direct evidence on this question comes from the experiments of Siegelbaum & Tsien (1980) who injected EGTA to abolish the internal $[Ca]_i$ transient and so record i_{si} in the absence of currents (such as i_{NaCa} and a component of i_{to}) dependent on $[Ca]_i$. The time constants for i_{si} in single ventricular cells have also been found to be very short, typical values being about 2–5 ms for activation and 10–20 ms for inactivation (Powell *et al.* 1981; Isenberg & Klöckner 1982; Lee & Tsien 1982; Mitchell *et al.* 1982; Mitchell *et al.* 1983). The equations we have used are:

$$\mathrm{d}d/\mathrm{d}t = \alpha_d\,(1-d) - \beta_d\,d, \tag{40}$$

$$\alpha_d = 30(E+24)/(1-\exp\,(-(E+24)/4)), \tag{41}$$

$$(\alpha_d)_{E=-24} = 120, \tag{41a}$$

$$\beta_d = 12(E+24)/(\exp\,((E+24)/10)-1), \tag{42}$$

$$(\beta_d)_{E=-24} = 120. \tag{42a}$$

These equations describe an activation process that has a 'threshold' near -35 mV, half activation at -24 mV and a peak time constant of about 5 ms.

$$\mathrm{d}f/\mathrm{d}t = \alpha_f(1-f) - \beta_f f, \tag{43}$$

$$\alpha_f = 6.25\ (E+34)/(\exp\ ((E+34)/4)-1), \tag{44}$$

$$(\alpha_f)_{E=-34} = 25, \tag{44a}$$

$$\beta_f = 50/(1+\exp\ (-(E+34)/4)). \tag{45}$$

These equations describe an inactivation process that is half-maximal at -34 mV (cf. Reuter *et al.* 1982) and has a peak time constant of about 20 ms. With these kinetics, i_{si} reaches a peak in less than 5 ms and is largely inactivated by 50 ms.

For the description of the Ca-dependent inactivation (see Brown *et al.* 1984*a*) we have used a formulation similar to that used recently by Standen & Stanfield (1982):

$$\mathrm{d}f_2/\mathrm{d}t = \alpha_{f2}(1-f_2) - \beta_{f2}[\mathrm{Ca}]_\mathrm{i} f_2 \tag{46}$$

which represents Ca-inactivation as occurring via a first-order binding reaction to the channel. In this equation, the speed of recovery from inactivation is determined by α_{f2}, its reciprocal being the time constant of recovery, which we usually set to 0.1 s. At the steady-state the degree of inactivation (that is, $1-f_2$) is given by:

$$1-f_2 = [\mathrm{Ca}]_\mathrm{i}/([\mathrm{Ca}]_\mathrm{i} + K_{\mathrm{m},f2}) \tag{47}$$

where $$K_{\mathrm{m},f2} = \alpha_{f2}/\beta_{f2}.$$

The value usually used for $K_{\mathrm{m},f2}$ was 1 μM which gives negligible inactivation at resting levels of $[\mathrm{Ca}]_\mathrm{i}$ but appreciable inactivation during the $[\mathrm{Ca}]_\mathrm{i}$ transient, as required if the experimental results are to be reproduced. An important result that is reproduced by this formulation is that i_{Ca} inactivation and recovery have quite different time constants even when measured at the same potential (see Brown *et al.* 1984*a*, figure 3).

We will show that, together with the equations for the exchange current, $i_{\mathrm{Na,\,Ca}}$, the equations reproduce the fast and slow components of i_{si} in Purkinje fibres (see figure 5 below) and in the s.a. node (see Brown *et al.* 1984*a*).

The question, though, remains whether there exists also a component corresponding to $i_{\mathrm{Ca,\,s}}$ in Purkinje fibres. This question will be explored in another paper (DiFrancesco *et al.* 1984).

(*j*) *Intracellular sodium concentration*

If we assume negligible binding of Na^+ ions the change in $[\mathrm{Na}]_\mathrm{i}$ will be given by:

$$\mathrm{d}[\mathrm{Na}]_\mathrm{i}/\mathrm{d}t = -(i_{\mathrm{Na}} + i_{\mathrm{b,\,Na}} + i_{\mathrm{f,\,Na}} + i_{\mathrm{si,\,Na}} + 3\,i_\mathrm{p} + (\mathrm{n}_{\mathrm{NaCa}}/(n_{\mathrm{NaCa}}-2))\ i_{\mathrm{NaCa}})/V_\mathrm{i}F \tag{48}$$

where V_i is the intracellular fluid volume.

Note that, strictly speaking, i_{Na} is not pure Na movement since we have assumed a 12% permeability to K^+ for the Na channel. The error this introduces is however very small. It would make a difference of less than 4% to the overall Na flux during an action potential. The reason for this is that the Na–Ca exchange process is at least as much involved in sodium entry as is the sodium current (DiFrancesco *et al.* 1985).

(*k*) *Intracellular calcium concentration*

Here we encounter the major difficulty in developing the model. It is clearly incorrect to assume that intracellular calcium is not bound. In fact, most of it is sequestered and the processes of sequestration are both complex and not very well understood. The approach we have adopted is to use the simplest possible equations to represent the essential features of the uptake and release processes from an electrophysiological point of view. Our aim has been to produce computed $[\mathrm{Ca}]_i$ transients that show a time course similar to that recorded in recent experiments (Allen & Kurihara 1980). Our assumptions are (see figure 1):

(i) The main sequestration store (which we shall refer to as the uptake store) is the sarcoplasmic reticulum. It is assumed that this occupies about 5% of the intracellular fluid volume and can sequester Ca^{2+} up to a concentration of 5 mM (Chapman 1979).

(ii) A fraction of the stored calcium is either transferred to a separate release store or is converted into a releasable form by a repriming process (cf. Hodgkin & Horowitz 1960). This process may be voltage dependent with a time constant of the order of a second or more at -80 mV (Gibbons & Fozzard 1975*a*, *b*).

(iii) Release of Ca^{2+} from the release store is induced by calcium (Fabiato & Fabiato 1975).

With these assumptions, the equations are:

$$i_{\mathrm{up}} = \alpha_{\mathrm{up}}[\mathrm{Ca}]_i\,([\overline{\mathrm{Ca}}]_{\mathrm{up}} - [\mathrm{Ca}]_{\mathrm{up}}) - \beta_{\mathrm{up}}[\mathrm{Ca}]_{\mathrm{up}}, \tag{49}$$

$$i_{\mathrm{tr}} = \alpha_{\mathrm{tr}}\,p([\mathrm{Ca}]_{\mathrm{up}} - [\mathrm{Ca}]_{\mathrm{rel}}), \tag{50}$$

$$i_{\mathrm{rel}} = \alpha_{\mathrm{rel}}[\mathrm{Ca}]_{\mathrm{rel}}\,([\mathrm{Ca}]_i^{\,r}/([\mathrm{Ca}]_i^{\,r} + K_{\mathrm{m,\,Ca}})) \tag{51}$$

where $[\overline{\mathrm{Ca}}]_{\mathrm{up}}$ is the maximum value of $[\mathrm{Ca}]_{\mathrm{up}}$, r is the number of Ca^{2+} ions assumed to bind to the release site (usually set to 2) and

$$\mathrm{d}p/\mathrm{d}t = \alpha_p(1-p) - \beta_p\,p. \tag{52}$$

This equation represents the time- and voltage-dependence of the exchange between storage and release sites. For the rate coefficients we used the same equations as for f slowed by a factor of 10. This gives the required steady state voltage dependence for the repriming process, which is similar to that for Ca current inactivation and reavailability. Then:

$$\mathrm{d}[\mathrm{Ca}]_{\mathrm{up}}/\mathrm{d}t = (i_{\mathrm{up}} - i_{\mathrm{tr}})/2V_{\mathrm{up}}F, \tag{53}$$

$$\mathrm{d}[\mathrm{Ca}]_{\mathrm{rel}}/\mathrm{d}t = (i_{\mathrm{tr}} - i_{\mathrm{rel}})/2V_{\mathrm{rel}}F, \tag{54}$$

$$\mathrm{d}[\mathrm{Ca}]_i/\mathrm{d}t = -(i_{\mathrm{si,\,Ca}} + i_{\mathrm{b,\,Ca}} - \{2i_{\mathrm{NaCa}}/(n_{\mathrm{NaCa}} - 2)\} + i_{\mathrm{up}} - i_{\mathrm{rel}})/2V_iF, \tag{55}$$

where V_{up} and V_{rel} are the volumes of the uptake and release stores respectively. The general features of this model are represented in figure 1.

The usual values used for the constants in these equations were as follows:

$[\overline{\mathrm{Ca}}]_{\mathrm{up}} = 5$ mM. This corresponds to the known Ca^{2+} sequestering ability of the sarcoplasmic reticulum (Chapman 1979).

$V_{\mathrm{up}} = 0.05\ V_i$, the reticulum is assumed to occupy 5% of the intracellular volume (Chapman 1979). Chapman's figure is for ventricular muscle. We have used the same parameter for the Purkinje model but it would clearly be desirable to replace this with an experimental value for Purkinje fibres.

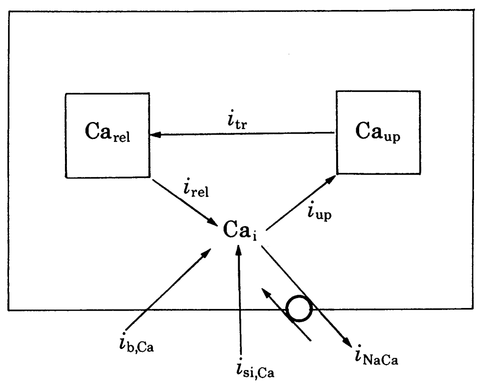

FIGURE 1. Diagram summarizing the processes assumed to control Ca^{2+} movements within the cell and across the cell membrane. An energy-consuming pump is assumed to transport calcium into the sarcoplasmic reticulum uptake store which then reprimes a release store. This may either be a physically distinct store or a releasable state of calcium within the same store. Release is assumed to be activated by cytoplasmic calcium ions. Ca^{2+} ions enter the cell through a background leak channel and through a gated channel. Ca leaves the cell through the Na–Ca exchange. Rarely it may enter through the exchange (for example, when $[Ca]_i$ is very low and the voltage very positive). These are the minimum assumptions required to model the $[Ca]_i$ transient. The model would need further development if it were thought necessary to add voltage-dependent Ca release, energy consuming surface membrane calcium pump, other calcium sequestration processes (such as binding to the contractile proteins), or further compartmentation of intracellular calcium.

$V_{rel} = 0.02\ V_i$. This figure is arbitrary and was chosen to give roughly the correct quantity of releasable calcium.

$K_{m,Ca} = 0.001$ mM when $r = 1$, 0.001^2 when $r = 2$. This figure is also somewhat arbitrary. Clearly, it cannot be as low as 0.0001 since resting calcium levels do not trigger release. 0.001 is sufficient to allow the quantity of calcium entering during an action potential to release stored calcium. The precise value of $K_{m,Ca}$ was not found to be important in the computations described in this paper.

The value of r was set to 1 or 2. The standard value was 2 since this gave oscillatory release (see DiFrancesco *et al.* 1983) more readily.

The rate coefficients were computed by the program from values set to the time constants of the processes involved. The release time constant, τ_{rel}, was set to 50 ms to enable $[Ca]_i$ to rise to a peak within 50 to 100 ms (Wier & Isenberg 1982; Allen & Kurihara 1980). The repriming time constant, τ_{rep}, was set to 2 s at -80 mV (Gibbons & Fozzard 1975*a*, *b*). The uptake time constant, τ_{up}, was set to 25 ms to allow uptake to occur sufficiently rapidly to reproduce the falling phase of the measured $[Ca]_i$ transients. This value also allows the s.r. to accumulate Ca^{2+} ions up to a concentration (about 2 mM) near half the maximum value (assumed to be 5 mM). These conditions are appropriate for a situation where the larger part of the $[Ca^{2+}]_i$ transient is due to internal cycling.

The values for the time constants were then used by the computer program to compute the rate coefficients using the relations:

$$\alpha_{up} = 2FV_i/(\tau_{up}\,[\overline{\mathrm{Ca}}]_{up}), \tag{56}$$

$$\alpha_{tr} = 2FV_{rel}/\tau_{rep}, \tag{57}$$

$$\alpha_{rel} = 2FV_{rel}/\tau_{rel}. \tag{58}$$

We should emphasize that this part of the modelling is not thought to be very secure. There are too many arbitrary factors and, in any case, the major issue of whether Ca^{2+} release is Ca^{2+}-induced or voltage-induced (or, perhaps, both) is still controversial. Our purpose here is therefore largely limited to reproducing the known $[Ca]_i$ transient time course. We have succeeded in doing this reasonably well, although we have not found it possible to reproduce the biphasic feature found by Wier & Isenberg (1982). We suspect that this would require further or different assumptions about intracellular calcium location and diffusion.

Despite the very tentative nature of the modelling of the $[Ca]_i$ transient, this feature of the model greatly extends its explanatory range since it is essential to model the $[Ca]_i$ transient in equations for Ca-dependent currents, like $i_{Na, Ca}$, $i_{Ca, f}$ and i_{to}. Even a primitive model, here, is much better than no model at all. An important consequence is that activity computed in this model is dependent on the inotropic state. This will be explored more fully in a subsequent paper (DiFrancesco *et al.* 1985).

(*l*) *Extracellular potassium concentration*

We assume that K^+ ions diffuse freely in the extracellular space so that we may use the free solution diffusion constant. In some calculations we have also assumed that there is a restriction factor that determines the degree to which free diffusion may be impeded.

The equation for diffusion in a cylinder where, at any point, ions may also cross the cell membrane, is

$$\partial[K]_c/\partial t = D\{\partial^2[K]_c/\partial x^2 + (1/x)\,\partial[K]_c/\partial x\} + i_{m, K}/V_e F \tag{59}$$

where

$$i_{m, K} = i_{K, 1} + i_K + i_{f, K} + i_{si, K} + i_{b, K} - 2i_p \tag{60}$$

and V_e is the extracellular space volume. For a cylinder this would be:

$$V_e = V_{ecs}\, a^2 l \quad \text{and, similarly,} \quad V_i = (1 - V_{ecs})\, V_e \tag{61}$$

where V_{ecs} is the fractional extracellular space (usually set to 5%), a is the radius and l the length of the preparation.

These are the equations we have used for calculations of $[K]_c$ in a Purkinje preparation when it has seemed important to represent the non-uniform distribution of extracellular K^+.

For a spherical preparation we have used the equation:

$$\partial[K]_c/\partial t = D\{\partial^2[K]_c/\partial x^2 + (2/x)\,\partial[K]_c/\partial x\} + i_{m, K}/V_e F \tag{62}$$

in place of (59).

Finally, for many purposes, we have found that the results are little affected by assuming a homogeneous K^+ concentration in a three-compartment model:

$$d[K]_c/dt = -P([K]_c - [K]_b) + i_{m, K}/V_i F \tag{63}$$

(cf. Attwell *et al.* 1979*b*), where $[K]_b$ is the bulk extracellular K^+ concentration and P is the rate constant for exchange between the bulk and cleft space. For most calculations we used values for P between 0.2 and 1.0 s^{-1}. This range of values was determined using a comparison between calculations using the cylindrical and three-compartment equations.

(m) *Intracellular potassium concentration*

This was computed by using:

$$\mathrm{d}[\mathrm{K}]_{\mathrm{i}}/\mathrm{d}t = i_{\mathrm{m,\,K}}/V_{\mathrm{i}}F. \tag{64}$$

Finally, it should be noted that we have used concentrations as synonymous with activities. This assumes that the intracellular and extracellular activity coefficients are very similar.

Methods

The set of equations (1–64) is extremely stiff since the range of time constants is exceedingly large. The sodium activation equation time constant is only of the order of 0.1 ms, whereas the equation for $[\mathrm{Na}]_{\mathrm{i}}$ has a time constant of the order of 5 min, a ratio of over a million. It is not therefore practical to use exactly the same numerical approach for all computations. With this and other requirements in mind a very general computer program, HEART, has been written which varies the computation methods to suit a wide variety of possible experimental situations. The ordinary differential equations were integrated using the methods described by Plant (1979). The partial differential equations, when used, were integrated separately using a method for inverting a band matrix of width three (see Modern computing methods 1961). Figure 2 shows a flow diagram of the main part of the program. The original programming language used for development was a version of Algol60 suitable for running on small machines. The program has subsequently been translated into Pascal. These languages were chosen for their superior logical structure compared with the Fortran IV available on PDP11 computers. The advantages that this gives in very large programs with extensive use of nested control loops were found to be very important in building-in the extreme flexibility which is one of the major features of the program. This readily permits new versions of the model (for example, for preparations other than the Purkinje fibre) to be incorporated as parameter procedures that set the constants and determine the pathway through the nested control loops. New control loops can also be added with ease since they do not refer to fixed labels. We have successfully run the Pascal version of the program using the RT11SJ monitor on PDP11/34 and PDP11/23 computers and the VMS monitor on a VAX computer. The program is extensively documented and no knowledge of Algol or Pascal is required unless substantial developments are envisaged, in which case an appropriate compiler will be required. A Pascal compiler for RT11 and other DEC systems is available from Oregon Software. The Pascal used is very close to the international standard, so that the program should easily transfer to other computers. Enquiries about the availability and use of the software should be addressed to Dr Noble.

Results and discussion

(a) *Current–voltage relations*

The steady state current–voltage relations given by the model can be analysed in the same way as those in the M.N.T. model (see McAllister *et al.* 1975, figures 2 and 3). The results obtained are not in general very different and will not be repeated here. Instead we shall describe new features that were not within the scope of the M.N.T. model.

First, we may now correctly describe the influence of extracellular potassium ions on the

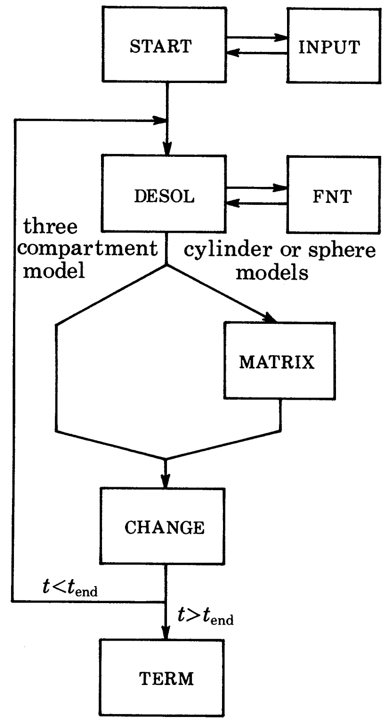

FIGURE 2. Flow diagram of the main features of the program. A procedure START either calls specific INPUT procedures containing parameters relevant to each preparation or version of the model, or reads a separate INPUT file. START then computes a variety of parameters that are used repeatedly in the computations and organizes output files. Each integration step then involves a call of the integration control procedure DESOL (see Plant 1979) which calls a number of other procedures, including FNT. The latter contains all the model equations and can readily be modified to produce new versions of the model. On exit from DESOL, procedure MATRIX is called to solve the diffusion equations when these are used. The three-compartment model bypasses this procedure. Procedure CHANGE controls the time changes of concentrations, currents, voltage clamp protocols etc. When t_{end} is reached, procedure TERM terminates the computation and tidies up the output files. This diagram shows only the main overall features. The program also contains about 20 other procedures not shown here which control an almost infinitely large number of modes of operation that can be tailored to the requirements of particular problems. The program is extensively annotated to enable these facilities to be operated without requiring any significant understanding of the program language.

current–voltage relations since all the known K^+-dependent processes are represented. Figure 3 shows the results of computing the quasi-instantaneous current–voltage relations at values of $[K]_b$ between 1 mM and 40 mM. It can be seen that the major features of the experimental results (see, for example, Dudel *et al.* 1967*b*; Sakmann & Trube 1984) are reproduced, including: (i) the presence of inward-going rectification with a negative slope region; (ii) the crossover of current–voltage relations at different values of $[K]_b$; (iii) the fact that at very low $[K]_b$ the net current–voltage relation becomes almost flat over a wide range of potentials; (iv) the presence of a net inward current region at low values of $[K]_b$.

The last feature was an important part of Noble & Tsien's (1969*a*) results and of their reconstruction of the plateau (Noble & Tsien 1969*b*).

The relations shown in figure 3 do not include the steady-state sodium current since the experiments of Dudel *et al.* (1967*a*, *b*) were performed in sodium-free (choline-substituted) solutions. It is however of interest to compare the results obtained including the steady-state sodium current since this has recently been measured experimentally by substrating current–

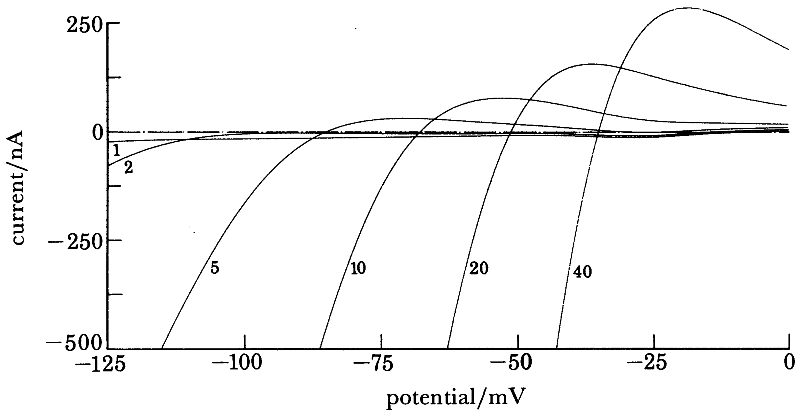

FIGURE 3. Steady-state current–voltage relations computed at various values of extracellular potassium concentration, $[K]_b$, from 1 to 40 mM. At each value of $[K]_b$ the model was clamped at −50 mV. Current–voltage relations were then computed assuming that the gating mechanisms *m*, *h*, *d* and *f* are held at their steady-state values at each potential, and that there are no significant variations in the Na–Ca exchange current. The last assumption is justified by our finding that the exchange system only carries large currents transiently and that these transients are quite fast when $[Ca]_i$ is in the diastolic range. This kind of result has been partly reconstructed by previous models (Noble 1965; Cohen *et al.* 1978). This is the first, though, to incorporate all the known $[K]_o$-dependent processes (i_{K1}, i_p and, to a lesser extent, i_K and i_{to}) with detailed experimental parameters.

voltage relations in the presence and absence of TTX (Attwell *et al.* 1979*a*; Colatsky & Gadsby 1980). Figure 4 (bottom) shows the 'window' current obtained from the model. This curve reproduces the experimental results fairly well. Attwell *et al.* (1979*a*) obtained a mean peak current value of −20 nA. The model gives −23 nA. The 'range' of the 'window' is about −60 to −20 mV which is closer to the experimental results than was the M.N.T. model. It is important to note that the 'window' current is well-reproduced even though our i_{Na} equations are based on Colatsky's (1980) results. The top part of figure 4 shows how our equations for *h* and m^3 fit Colatsky's data. There is only very little overlap between m^3 and *h* but this is sufficient to generate a 'window' current that only needs to be less than 1% of the peak i_{Na}.

(*b*) *Reconstruction of voltage clamp currents*

Figure 5 shows the extent to which the equations can reproduce the voltage clamp results obtained in Purkinje fibres with regard to the fast calcium current, slower inward current and the transient outward current. Traces (*a*) to (*f*) show currents computed on voltage clamping from −80 mV to the potentials shown. In each case the current was computed for the standard case with g_{Na} set to zero (that is, TTX block of g_{Na} is assumed), and then with i_{to} and i_{NaCa} set to zero to eliminate the current dependent on the $[Ca]_i$ transient. This was done to mimic the situation in Siegelbaum & Tsien's (1980) experiments where the $[Ca]_i$ transient was eliminated by EGTA injection. Record (*f′*) shows the computed $[Ca]_i$ transient corresponding to (*f*). Record (*a′*) shows the result of changing from −50 mV to −40 mV. The reason for this additional record will become clear later. Finally, records (*g*) and (*h*) show experimental records chosen for comparison with computed records (*a*) and (*e*), (*f*).

First, it is worth noting that the amplitudes and speeds of i_{si} and i_{to} at potentials near 0 mV correspond well with those in Siegelbaum & Tsien's (1980) results. Moreover, when i_{to} is blocked the peak inward current level is increased and the current record becomes much

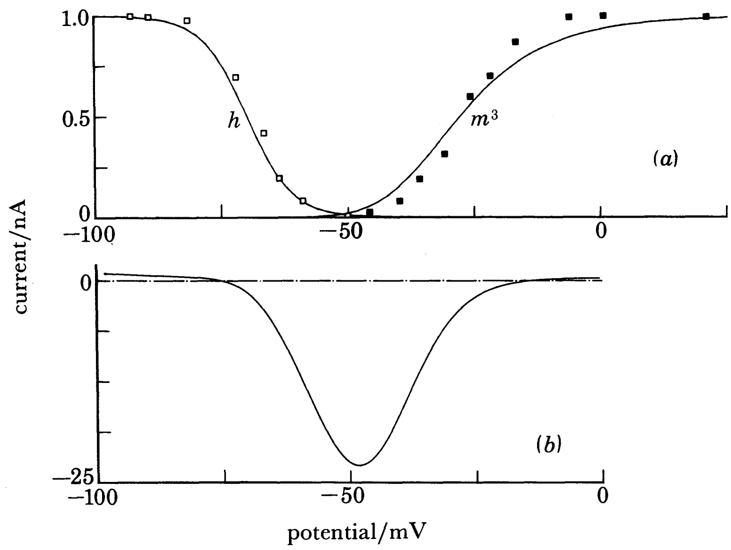

FIGURE 4. (*a*) Points show experimental data (Colatsky 1980) on the activation (■) and inactivation (□) of the sodium current in Purkinje fibres. The continuous lines show the steady state values of m^3 and h given by the model. Note that we have fitted the h data fairly accurately, but have chosen a somewhat less steep function for m^3. In this choice we were influenced by the data on single cells (Brown *et al.* 1981) showing an activation curve similar in steepness to our equations. This choice also allows a better reconstruction of the 'window' current. (*b*) 'Window' current computed by subtracting current–voltage relations obtained before and after setting g_{Na} to zero. This curve is similar to that obtained experimentally. The small outward current shift negative to −75 mV is due to a small change in the Na gradient when g_{Na} is blocked. Note that the 'overlap' region shown in (*a*) appears to be a very small region near −50 mV. The curve in (*b*) shows that, when dealing with very small currents, the overlap is more extensive at values of m^3 and h that are too small to appear significantly different from zero in the top curves.

simpler. The records before and after removing $[Ca]_i$-dependent currents cross each other as they do in the experimental results. In the model this is due to the presence of a long-lasting small inward current caused by Na–Ca exchange. The main difference between the computed and experimental results here is that the difference persists to much longer time in the experimental results. This might be due to the presence of a genuine slow Ca current, $i_{Ca,s}$, (Lee *et al.* 1984*a*) if that current is $[Ca]_i$-dependent. We will return to these differences later in discussing figure 6.

Turning now to the voltages below the range of activation of i_{to}, it is clear that near −40 mV a very slow inward transient occurs that lasts about 500 ms. Its amplitude and duration are similar to those of the current recorded at −40 mV by Eisner *et al.* (1979) – see also Lederer & Eisner (1982) – which is shown as record (*g*). Also shown is the effect of caffeine at a level thought to discharge the s.r. This removes the current, as does removal of transient changes in i_{NaCa} in the model. Of course, caffeine should first itself induce an inward current while the stores are being discharged. Clusin *et al.* (1983) have recently described just this effect in embryonic heart cells. They also attribute the current to the Na–Ca exchange process.

The main differences between traces 5*a* and 5*g* is that the computed response has a sharper onset compared to its decay. It is worth noting that this may also occur experimentally (see, for example, Lederer & Eisner 1982, figure 2). In our equations, this feature depends on the current magnitude: the onset is faster the larger the current (see also Brown *et al.* 1984*a*). Another feature worth noting is that Siegelbaum & Tsien's (1980) results do *not* show this very slow current in the region of −40 mV. The reason may be that they used a holding potential

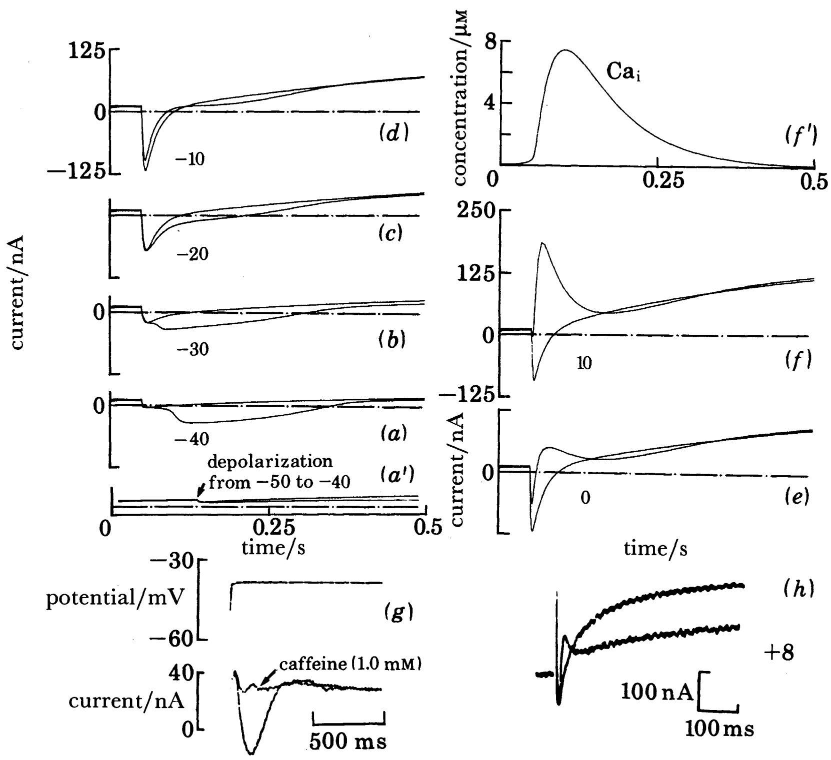

FIGURE 5. Voltage clamp currents computed from the model. In records (*a*) to (*f*), the voltage was stepped from −80 mV to the potentials indicated, first using the full equations (with g_{Na} set to zero) and then with i_{to} and i_{NaCa} also set to zero to mimic the expected result of eliminating the currents dependent on $[Ca]_i$. Record (*f′*) shows the intracellular Ca transient computed during record (*f*). Record (*a′*) shows the effect of changing the holding potential to −50 mV. The very slow inward current seen on clamping to −40 or −30 from −80 mV is then no longer seen. Records (*h*) show superimposed experimental records from Siegelbaum & Tsien (1980). They clamped from −45 mV to, in this case, +8 mV. Record (*g*) shows experimental records from Eisner *et al.* (1979). Note that the time scales for the experimental records are not the same as those for the computed records. See text for further description.

around −45 mV. It is important to note (see record (*a′*)) that in the model also, holding at, in this case, −50 mV eliminates the slow component. This is because little Ca release occurs on depolarizing from −50 to −40 mV.

In single guinea-pig ventricular cells a similar situation is found to occur. Depolarizations from −80 mV to −50 mV produce a slow component of current (see Lee *et al.* 1983) whereas depolarizations from −50 mV to −40 mV or −30 mV fail to trigger this component.

This is a suitable point at which to comment on the diversity of the experimental information concerning the slower components of i_{si} (see also review by Noble 1984). The range is so wide that, in some experiments, currents like that shown in figure 5*a* and 5*g* are apparently not observed at all. It is important to note that this is quite consistent with the system of equations we have described. To ensure the apparent absence of the slow component, it is sufficient to reduce a little the sensitivity of the Ca-release mechanism to intracellular calcium (by increasing $K_{m,\,Ca}$). Transients due to i_{NaCa} are then always greatly masked by the activation of the much larger $i_{Ca,\,f}$, combined with the fact that the onset of i_{NaCa} is then also much faster. An example of this behaviour is shown using the sinoatrial node version of the model in Brown *et al.* (1984*a*, figure 10*a*), where the computed time course of i_{si} decay is clearly monotonic.

(c) *Standard action and pacemaker potentials*

Figure 6 shows the standard action potential and intracellular Ca^{2+} transient computed at $[K]_b = 4$ mM. To induce pacemaker activity the *y* variable was shifted 10 mV in a positive direction (cf. Hauswirth *et al.* 1968). The intracellular Ca^{2+} transient rises to a peak within about 50 ms and decays well before the faster phase of repolarization begins. This corresponds

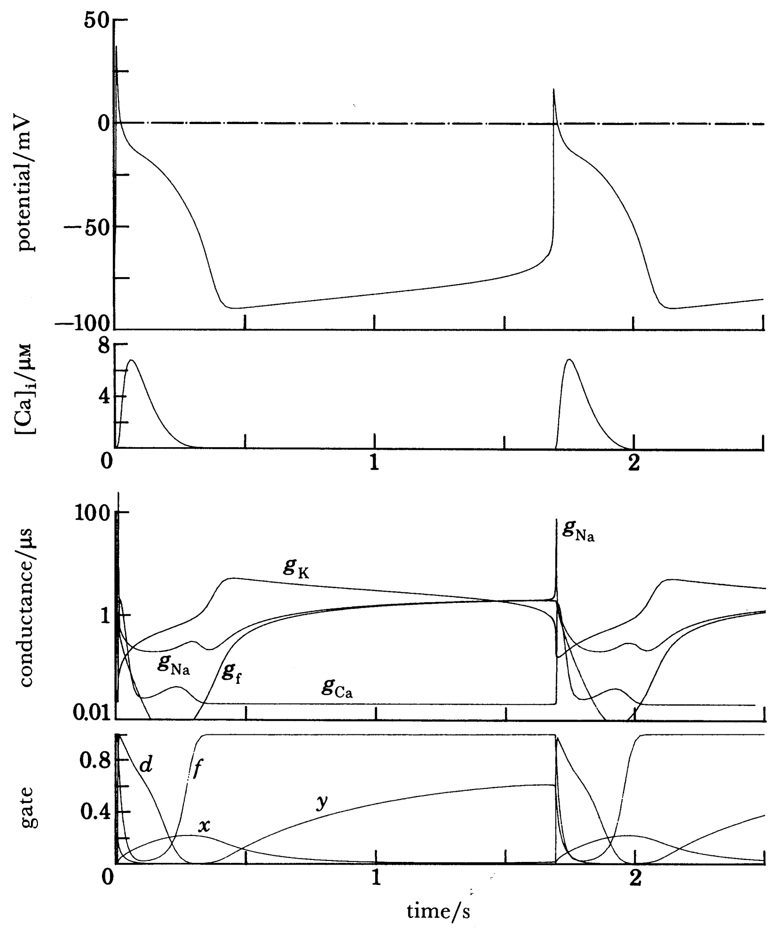

FIGURE 6. Standard action potential, pacemaker potential, intracellular calcium transient, conductances (on a logarithmic scale) and gating variables computed for $[K]_b = 4$ mM. Description in text.

well to the experimental results with aequorin, except that we do not find the biphasic response seen by Wier & Isenberg (1982) in Purkinje fibres. In principle, two peaks are possible in the model since the Ca^{2+} transient is made up of two components: a smaller one due to the calcium current and a larger one due to internal release. In practice, these fuse together as they appear to do experimentally in ventricular muscle. We do not know whether any of the electrophysiological phenomena dependent on intracellular calcium depend on the biphasic response, but we suspect that the time course reproduced in figure 6 is a good first approximation.

The lower part of figure 6 shows the computed conductance changes plotted on a logarithmic scale. In this diagram 'g_K' includes the conductances (computed as chord conductances) due to i_{K1}, i_K and $i_{f,K}$; 'g_{Na}' includes the conductances due to i_{Na}, and $i_{f,Na}$; 'g_{Ca}' includes those due to $i_{Ca,f}$ and $i_{b,Ca}$, while 'g_f' is the sum of $g_{f,Na}$ and $g_{f,K}$. Our reason for using these combinations is that, apart from g_f, they correspond most closely to the equivalent parameters in the M.N.T. model.

It can be seen that the variations in the equivalent conductances show some resemblance to those in the M.N.T. model. In particular, the K^+ conductance time course is almost identical to that of the M.N.T. model. The other conductances, however, show significant differences. The main differences are: (i) the decay of g_{Ca} is very much faster, and (ii) the onset of g_f during the pacemaker depolarization is a new feature that was not present in the M.N.T. model which represented the equivalent process as the decay of a specific K^+ conductance. The reason for the close resemblance for the remaining terms included in 'g_K' is that by far the largest factors in the time course of 'g_K' in the M.N.T. model and in the new model are the voltage-dependent variations in $i_{K,1}$ and the time and voltage dependent variations in i_K (the formulations of which are very similar in the two models). Another way of demonstrating these features of the model is to measure 'slope' conductance as it would be measured experimentally by applying small repetitive voltage pulses (as shown in DiFrancesco & Noble 1982). The results reproduce Weidmann's (1951) data despite the radical re-interpretation of i_{K2} (for further discussion of this and related results see DiFrancesco & Noble (1982)).

The importance of the hyperpolarizing-activated current, i_f, in the pacemaker depolarization may be demonstrated by computing the effects of shifting the voltage dependence of the gating variable to reproduce the effects of adrenaline (Hauswirth *et al.* 1968; Tsien 1974; Hart *et al.* 1980). With $[K]_b = 2.7$ mM, a 15 mV shift is sufficient to double the firing frequency. A 30 mV shift leads to substantial depolarizaton. If g_{si} is increased the result is very rapid pacemaker activity of the kind seen experimentally after strong doses of adrenaline. The results are so similar to those illustrated by McAllister *et al.* (1975) that we have not shown them as a figure in this paper.

Figure 7 shows the time courses of the main current components. For clarity, the fast sodium current has been omitted (its time course can be estimated from the conductance changes plotted in figure 7).

While i_f is the main time-dependent gated current that contributes to pacemaker activity, other currents also contribute substantially. The net increase in i_f during the pacemaker depolarization in figure 8 is -14 nA. By comparison, i_K shows a fall of 5 nA during the pacemaker potential; $i_{b,Na}$ carries a roughly constant -26 nA, $i_{b,Ca}$ carries about -10 nA, i_{NaCa} carries about -4 nA and the sodium–potassium exchange pump carries about 17 nA. The difference is made up by i_{K1} which carries about 31 nA.

(*d*) *Influence of external* [K] *on action potentials and pacemaker activity*

Figure 8 shows the influence of varying the bulk extracellular K^+ concentration. At 12 and 20 mM the action potential is of fairly brief duration and a stable resting potential is established immediately following repolarization. Decreasing $[K]_b$ to 8 or 6 mM lengthens the action potential, hyperpolarizes the membrane and, in consequence, activates i_f to produce a pacemaker depolarization, though at these concentrations the depolarization is insufficient to reach the action potential threshold. At 4 mM slow repetitive firing occurs. Further reduction to 2.7 mM lengthens the action potential even further and the pacemaker potential becomes much steeper. These are the well-known effects of external [K] on action potentials and

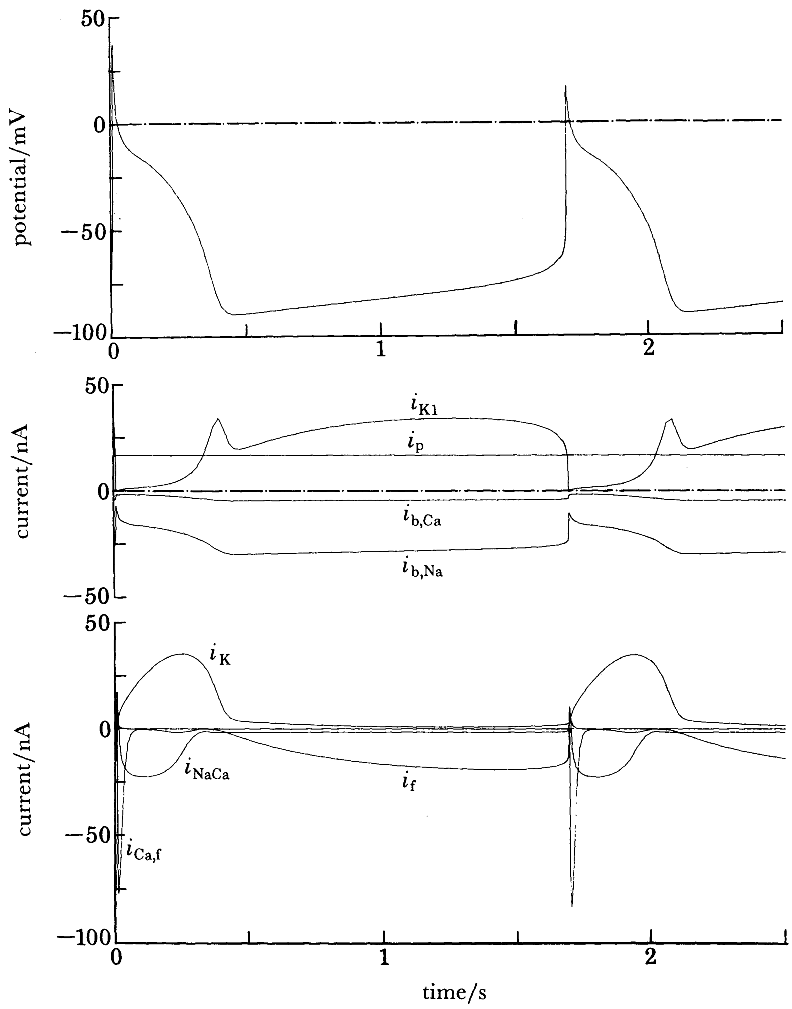

FIGURE 7. Continuation of figure 6. This shows ionic currents (except for i_{Na} which is too large for the current scale used here).

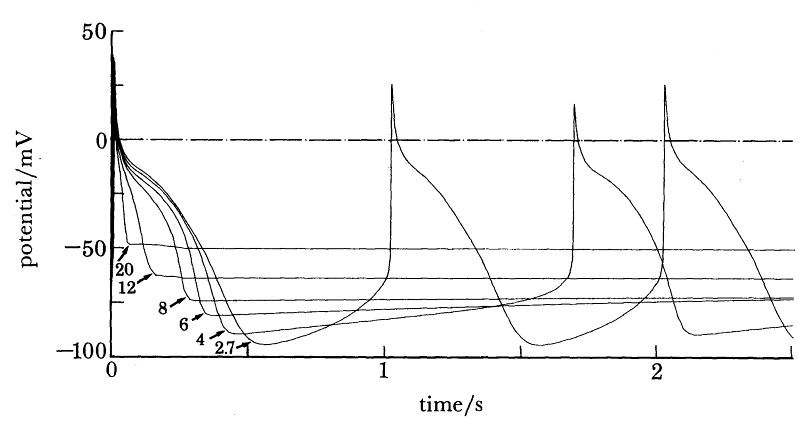

FIGURE 8. Influence of extracellular [K] on action and pacemaker potentials. Description in text.

pacemaker activity in Purkinje fibres (Weidmann 1956; Vassalle 1965). At values below 2.7 mM, the behaviour depends critically on the value assumed for the background sodium conductance $g_{b,Na}$. With this conductance set at 0.02 μS, the model fails to repolarize at very low [K] and, after a damped oscillation, the membrane potential settles at −40 mV. This effect is shown in Noble (1984, figure 4) and corresponds to the well-known depolarizing effect of very low [K] in Purkinje fibres (Weidmann 1951; Gadsby & Cranefield 1977).

(e) *Influence of external* [Na] *on action potentials, pacemaker activity and intracellular sodium*

In 1951, Draper & Weidmann described the influence of $[Na]_o$ on the overshoot and pacemaker activity in Purkinje fibres. The overshoot potential was found to follow closely the behaviour of a sodium electrode, while the duration of the plateau and the rate of pacemaker depolarization were both greatly reduced in low $[Na]_o$. At the time these results appeared they were taken at face value as strong support for the application of the Na hypothesis (Hodgkin & Katz 1949) to the heart, and as support for a role of Na ions in the pacemaker depolarization.

More recent experiments, however, have made Draper & Weidmann's work seem less simple than when it first appeared. When $[Na]_o$ is changed $[Na]_i$ changes fairly rapidly, the time constant of change being about 3 min (Ellis 1977; Sheu & Fozzard 1982). Moreover, the change in $[Na]_i$ is almost linearly proportional to the change in $[Na]_o$ with the consequence that E_{Na} changes by very much less than 61 mV per tenfold change in $[Na]_o$. In fact a tenfold decrease in $[Na]_o$ would be expected to produce less than 30 mV change in E_{Na}. This raises the question how Draper & Weidmann could possibly have obtained such an apparently simple result for the overshoot potential.

The answer may be provided by the second complication, which is that the value of E_{Na} predicted from intracellular Na measurements is about 30–40 mV positive to the observed overshoot potential. Thus, with $[Na]_i$ in the range 4–10 mM (which is fairly typical) and $[Na]_o$ at 140 mM, E_{Na} is expected to be about 70–100 mV, whereas the overshoot is only about 30–40 mV.

The explanation for the last result is fairly obvious: the 'Na' channel may not exclude other ions. Indeed, in our equations, we have allowed for this by using the result obtained in squid nerve (Chandler & Meves 1965) showing a 12% permeability to K^+ ions in the 'Na' channel. The reversal potential is then given by equation (29), which since 0.12 $[K]_c$ is very small compared to $[Na]_o$ simplifies to:

$$E_{mh} = (RT/F) \ln ([Na]_o/([Na]_i + 0.12\,[K]_i)) \tag{65}$$

and, since $[K]_i \gg [Na]_i$, E_{mh} would be expected to be relatively insensitive to $[Na]_i$.

First, we checked whether the equations can reproduce the $[Na]_o$-dependence of $[Na]_i$. The results are shown in figure 9. When $[Na]_o$ is reduced, $[Na]_i$ falls in an almost exponential manner with a time constant (3.3 min) that is very close to Ellis's (1977) experimental value (see also Sheu & Fozzard 1982; Chapman *et al.* 1983). Moreover, over a wide range of concentrations, $[Na]_i$ is almost linearly proportional to $[Na]_o$, as shown in figure 10. We then used these values of concentrations to investigate the $[Na]_o$-dependence of the computed overshoot potential. The results are shown in figure 11 and clearly closely follow Draper & Weidmann's results. Moreover, as found by them, the 'fibre' becomes inexcitable below about 15 mM $[Na]_o$. We also found the pacemaker depolarization to be less evident and the action potential duration reduced (not shown here). The latter effect is in part attributable to the contribution of the

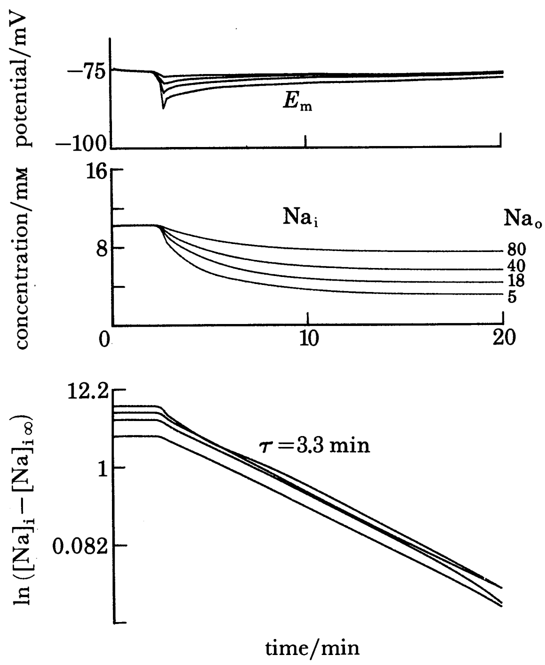

FIGURE 9. Influence of $[Na]_o$ on membrane potential and on intracellular $[Na]_i$. $[Na]_o$ was reduced from 140 mM at time 2 min to 80, 40, 18 or 5 mM at time 2.5 min. There is a transient hyperpolarization similar in amplitude and duration to that seen experimentally (Ellis 1977). In the model this is attributed to a reduction in i_{NaCa} while the Na gradient is reduced. Note that this effect is largely transient. The bottom diagram shows the $[Na]_i$ changes plotted on a semilogarithmic scale. $[Na]_i$ falls exponentially with a mean time constant of 3.3 min.

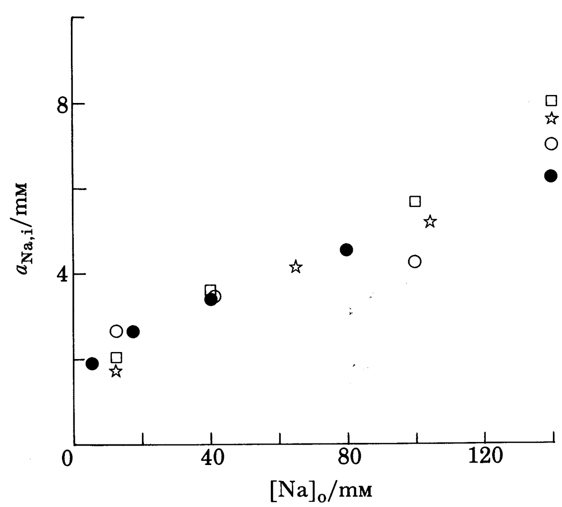

FIGURE 10. Steady-state variation of $a_{Na,i}$ with $[Na]_o$. The open symbols show results replotted from Ellis (1977). The closed symbols show the model's predictions using an activity coefficient of 0.75. In both experimental and computed results there is a roughly linear variation of $[Na]_i$ with $[Na]_o$. (See also Chapman *et al.* 1983.)

Na 'window' current to the plateau and in part to entry of Na by the Na–Ca exchange mechanism.

The suppression of pacemaker activity in low $[Na]_o$ requires further comment. It might be thought that this represents the contribution of the sodium background current to the pacemaker depolarization. This is not so since we have assumed (see above) that the Na

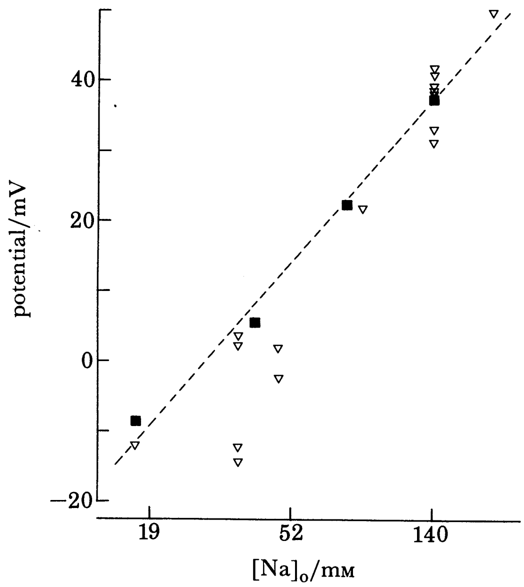

FIGURE 11. Variation of overshoot potential with $[Na]_o$. The open triangles are results replotted from Draper & Weidmann (1951). The closed squares show the model's predictions. The interrupted line shows a 61 mV variation per decade change in $[Na]_o$. Below 15 mM the model, like the real fibres, is inexcitable.

replacement can also pass through the background channel (Na replacement by choline, for example, does not greatly alter the resting potential in Purkinje fibre – see Hall *et al.* 1963). The reduction in the rate of the pacemaker depolarization is in fact attributable to the fact that, in the pacemaker range of potentials, i_f is largely carried by Na ions. Draper & Weidmann (1951) actually gave as one of their explanations the view that 'the slow depolarization during diastole...depends on the entry of sodium'. For the Purkinje fibre, on the new interpretation of i_{K2}, this is entirely correct even during the early phase of the pacemaker depolarization. As in the M.N.T. model, the later part of the pacemaker depolarization is also dependent on a small degree of activation of the fast sodium current. All the conclusions drawn by McAllister *et al.* (1975) on this point apply equally well to the new model, including their explanation for the influence of surface charge changes due to calcium ions.

One way of demonstrating the role of the fast sodium current is to compute the effects of reducing g_{Na}. This is shown in figure 12. As in Coraboeuf & Deroubaix (1978) and Colatsky's (1982) recent experimental work, this produces a marked shortening of the action potential and pacemaker activity is suppressed by reducing the rate of depolarization in the later phase.

(*f*) *Ionic current changes due to the* Na–K *pump*

The current carried by the Na–K pump has been extensively investigated recently. A standard method (used both by Gadsby and by Eisner & Lederer) has been to place a preparation in a K-free solution for several minutes to reduce pump activity and so to increase $[Na]_i$. The preparation is then returned to a K^+-containing solution. An outward current transient is then recorded as the increased internal sodium stimulates the pump. An example of this kind of experiment and its reconstruction is shown in figure 13. The top records are reproduced from Gadsby (1980) and show currents in a dog Purkinje fibre following various periods of K-free superfusion for up to 3 min. The middle record shows the computed result from the model with the variations in cleft [K] and $[Na]_i$ shown below. The computed variation

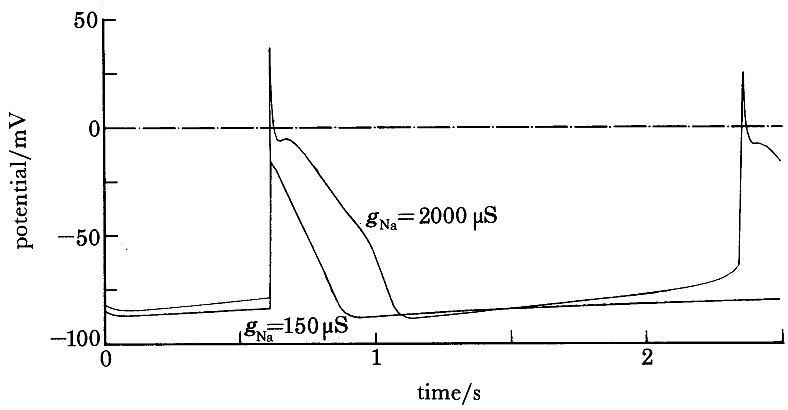

FIGURE 12. Influence of decreased g_{Na} on action potential and pacemaker activity. g_{Na} was reduced from 2000 μS to 150 μS. This abolishes the spike of the action potential and eliminates pacemaker activity. The effect on the action potential duration illustrates the role of the sodium 'window' current in the plateau.

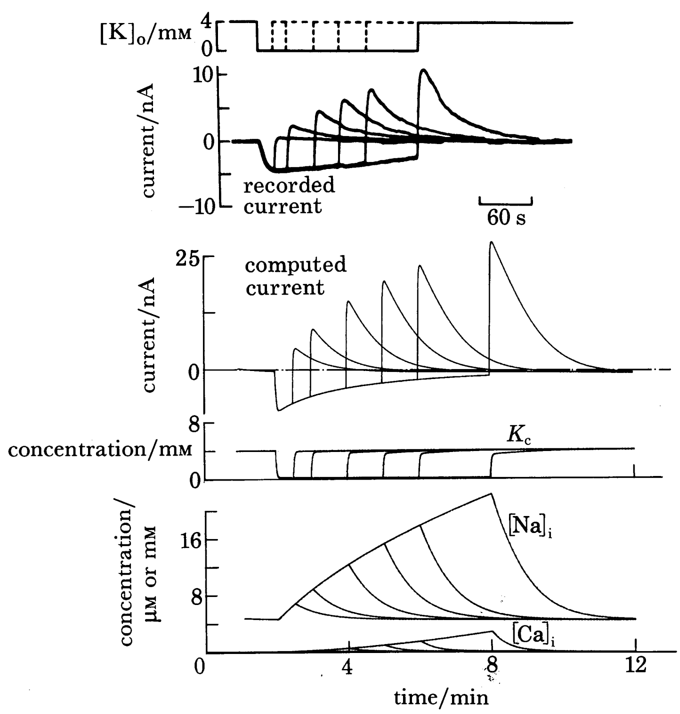

FIGURE 13. (*a*) Experimental records of changes in ionic currents in response to changes in $[K]_b$ in a canine Purkinje fibre (from Gadsby 1980). (*b*) Computed variations in ionic current and in $[K]_c$. (*c*) Computed variations in $[Na]_i$ (in millimoles per litre) and in $[Ca]_i$ (in micromoles per litre).

in $[Na]_i$ corresponds well to Ellis (1977) and Deitmer & Ellis's (1978) measurements showing that in K^+-free medium $[Na]_i$ doubles in a period of about 5 min. The computed increase in $[Ca]_i$ (also shown) corresponds well to the fact that tonic tension is known to increase over this period of time, and Sheu & Fozzard (1982) have recently recorded $[Ca]_i$ with a calcium electrode showing changes comparable to those computed here.

We think, therefore, that we can have some confidence in the model's predictions concerning the intracellular concentration changes during K-free inhibition of the pump.

We turn now to the reconstruction of Gadsby's ionic current measurements. It can be seen that the computed results show a very similar pattern. Not only does the model correctly reproduce the outward current transients on return to K^+-containing solution; it also reproduces the slow upward current creep that occurs while the preparation stays in the K^+-free medium. The model provides a possible explanation for this phenomenon, which is that, although we have assumed a large extracellular cleft space (30% in this case) the cleft K^+ concentration does not fall to the bulk K^+ concentration since it takes time for diffusion to occur. This allows a residual degree of K^+ activation of the pump, which is then further activated as $[Na]_i$ increases, so producing the upward current drift.

Mullins (1981) has proposed an alternative explanation in terms of the Na–Ca exchange current. We can exclude this explanation since on the time scale of this kind of experiment the Na–Ca exchange system will be close to its steady-state activity at nearly all times. If the background Ca influx remains constant and small, there is no reason why the Na–Ca exchange current should vary greatly.

This is perhaps a suitable point at which to emphasize a general result we have found with the model: this is that the Na–Ca exchange current is nearly always very small (about 4–5 nA, that is, much smaller than the Na–K pump current) in the steady-state. Large currents are carried by the exchange process only as transients. When $[Ca]_i$ is very low (less than 0.1 μM) these transients are very rapid (a few milliseconds); when $[Ca]_i$ is large (for example, 5 μM) the transients can last several hundred milliseconds (as during a computed action potential – see figure 7).

The magnitude of the upward current drift is somewhat larger in the model than in Gadsby's result. This amplitude is strongly dependent on the size of the extracellular space and on the time constant for cleft-bulk space diffusion. A shorter time constant for the diffusion process would give a smaller current creep.

We conclude that the model does accurately reproduce current changes due to Na–K pump activity. We will now use the model to investigate two other kinds of experiment in which the influence of pump changes has been measured.

Figure 14 shows the influence of the Na–K pump activity on the duration of the action potential. This computation is designed to reproduce Gadsby's (1982) measurements of the

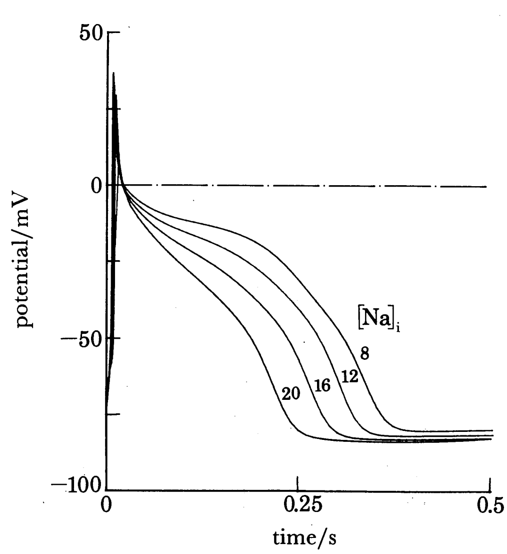

FIGURE 14. Action potentials computed at various values of $[Na]_i$ between 8 and 20 mM.

shortening of the action potential on return to K^+ containing solutions after a period of several minutes in K^+-free solution. We computed the standard action potential in 6 mM K^+ at various values of $[Na]_i$ between the normal level of 8 mM and up to 20 mM. This is the range of $[Na]_i$ increase expected during several minutes exposure to K^+-free solution. The shortening of the action potential is similar to that recorded experimentally. Notice also the small hyperpolarization in the resting state, which is also seen experimentally.

The computations on the influence of the Na–K pump described so far were done with large extracellular space volumes appropriate to the known structure of canine Purkinje fibres. We now turn to the possible effects of more restricted spaces such as are found in sheep Purkinje fibres.

Figure 15 shows the results computed on return to a range of external activator cation

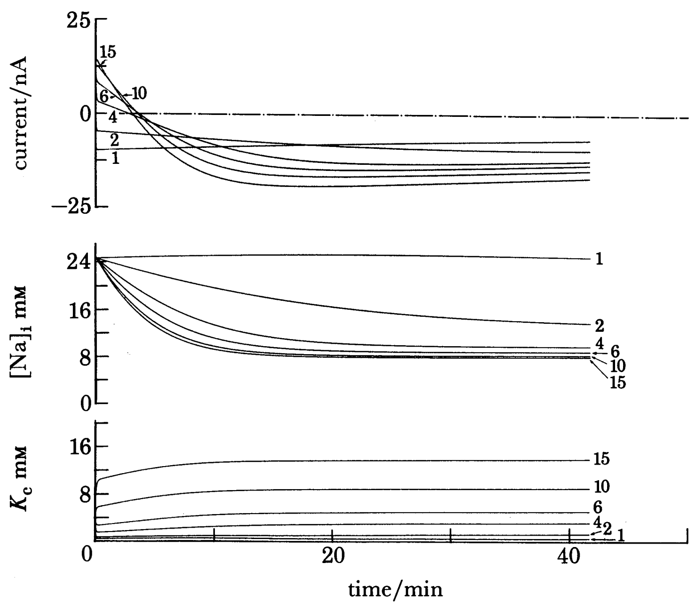

FIGURE 15. (a) Computed ionic currents following reactivation of the Na–K pump by various concentrations of external activator cation (1–15 mM) after allowing $[Na]_i$ to rise to 25 mM blocking Na–K pump. (b) Corresponding variation in $[Na]_i$. (c) Corresponding variations in $[K]_c$.

concentrations between 1 and 15 mM after a period of K-free superfusion leading to an increase in $[Na]_i$ to 25 mM. For these computations we used a cleft space volume of 5 % and a diffusion time constant of 5 s. These parameters are interrelated. A smaller cleft volume together with a shorter diffusion time constant would give similar results. We have also run some computations using the full diffusion equations for a two-dimensional cylindrical space. The results are similar to those shown in figure 16, but each case takes much longer (several hours instead of a few minutes) to compute. Finally, since these computations were designed to reproduce the experimental conditions investigated by Eisner & Lederer (1980), in which Rb was used in place of K as the activator cation to reduce the effects of K depletion by reducing the inward rectifier current, we reduced g_{K1} to 5 % of its usual value.

The top traces in figure 15 show the net ionic current changes. It can be seen that at 1 mM Rb (Rb and K are roughly equipotent activators of the Na–K pump) there is virtually no current transient. Eisner & Lederer (1980) also found only a very small current at 1 mM. A comparable computation using a 30% cleft volume gave a nearly 50% activation of the pump (as expected since the 'true' K_m assumed in these computations is 1 mM). 2 mM produces a small slowly declining current transient. As much as 4 mM is required to activate 50% of the maximum current and speed of current change, which is not reached until the activator cation concentration is increased above 10 mM. This corresponds quite closely to Eisner & Lederer's curve for activation of the pump current by external cation, giving an apparent K_m in the region of 4–5 mM, despite the fact that the true value is 1 mM.

We found the apparent K_m value to be strongly dependent on the extracellular space size and the assumed diffusion time constant. It is easy to obtain apparent K_m values as high as 10 mM by halving the space size or increasing the diffusion time constant. With cleft spaces less than about 1–2% it becomes almost impossible to deactivate the pump in low $[K]_b$. Thus the high apparent value of K_m is attributable to the 'inertia' of the cleft system in relation to bulk [K] changes.

There may appear to be a difficulty, though, with this explanation. This is that Eisner *et al.* (1981) were careful in their experiments to check that the pump current change is linearly dependent on $[Na]_i$. This is the result they found over the range of $[Na]_i$ values between 8 and 16 mM. As they point out, a large effect of external cation depletion on the pump activity might upset this linearity.

Nevertheless, we don't find this effect to be very significant. Figure 16 shows our results

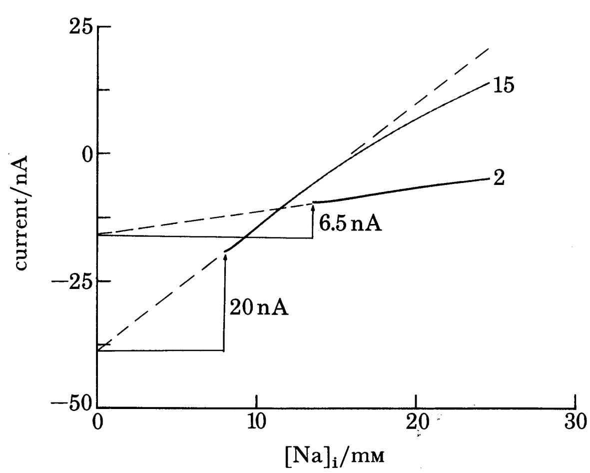

FIGURE 16. The results of figure 15 are replotted as current–$[Na]_i$ relations as they change during pump reactivation at various concentrations of activator cation. When the activator cation is 2 mM there is a nearly linear relation over the whole range. At 15 mM the result is nearly linear over the range of $[Na]_i$ between 8 and 16 mM. The extrapolated lines show how the current at $[Na]_i = 0$ can be estimated, as done by Eisner *et al.* (1981) to estimate the resting pump current.

replotted as current-$[Na]_i$ curves. With activation by 2 mM external cation, the result is close to linear over the whole range. With 15 mM external cation concentration the curve is close to linear over the range 8–16 mM but deviates from linearity above this range. Thus, over the relevant range of the experiments, a nearly linear relation is obtained. Furthermore, the computed deviation from linearity above 16 mM is almost entirely attributable to the arbitrary value of 40 mM assumed for the K_m for internal Na activation of the pump. If this is increased to, say, 100 mM the results are linear up to much larger Na^+ concentrations.

Further results related to i_p and consequential changes in $[Na]_i$, $[K]_c$ and in current–voltage relations have already been published by Hart *et al.* (1983).

(g) *Current changes formerly attributed to* i_{K2}

We have already given a fairly complete treatment of this question using an earlier, and much simpler, version of the model (DiFrancesco & Noble 1982). Here we will restrict ourselves to showing that essentially the same results are obtained with the more complete version described in the present paper.

Figure 17 shows ionic currents and mean cleft K^+ concentrations computed using the

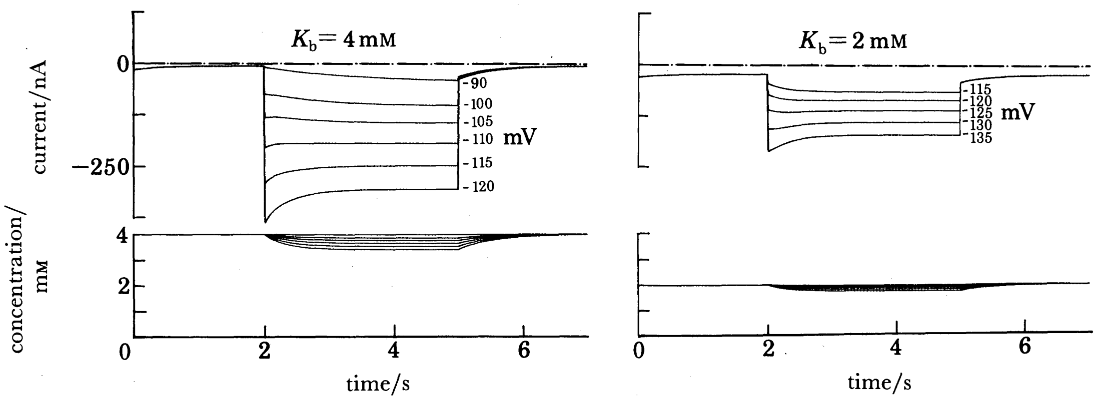

FIGURE 17. Examples of currents computed in response to hyperpolarizations from −50 mV to various potentials in the activation range for i_f. The extracellular cleft space was set to 10% and the full cylindrical diffusion equations were used to estimate the K concentration profiles as a function of radial distance. Below each set of current records we show the mean values of $[K]_c$. At $[K]_b = 2$ mM there is a reversal of total time-dependent current between −125 and −130 mV. At $[K]_b = 4$ mM the reversal occurs at about −110 mV. Similar results have been obtained for extracellular space volumes between 0.5 and 30%. For further analysis of the influence of extracellular space volume, see DiFrancesco & Noble (1982).

diffusion equations for a cylindrical space. The space volume was set to 10% and step hyperpolarizations were imposed from −50 mV to the potentials indicated. A variety of bulk extracellular K^+ concentrations was used. The results for 2 mM and 4 mM are illustrated. Note that at each value of $[K]_b$ there exists a potential at which the net time-dependent current change changes direction. As shown in our previous work (DiFrancesco & Noble 1980*c*, 1982) this reversal, although it often gives the appearance of a simple single component (which is what led to its identification in experimental work as a true ionic channel reversal potential) is in fact attributable to a balance between an inward current change due to the activation of i_f during hyperpolarizations and an outward current change due to a decrease in inward-flowing i_{K1} during depletion of K^+ ions from the cleft space. The time constants for these two processes are sufficiently close under most circumstances to produce the impression that a single component (perhaps slightly perturbed by depletion) is responsible. It is noteworthy that the amounts of K^+ depletion required to produce this effect are very small. Typically a reduction of only 0.5 mM in the mean $[K]_c$ is sufficient to generate a change in i_{K1} sufficient to mask the opposite change in i_f. This decrease in mean $[K]_c$ only represents a change of 10% at $[K]_b = 5$ mM. The reduction in the total i_f conductance – which is

K-activated (see DiFrancesco 1982) – during large hyperpolarizations may further contribute to the observed reversal effect.

There is some argument about the precise size of the extracellular space (see, for example, Cohen *et al.* 1983). We have therefore repeated these computations over the range 0.5–30%. The same kind of result is obtained in all cases. The influence of space size on E_{rev} is treated fully in DiFrancesco & Noble (1982).

Figure 18 shows the variation in reversal potential as a function of external [K] on a

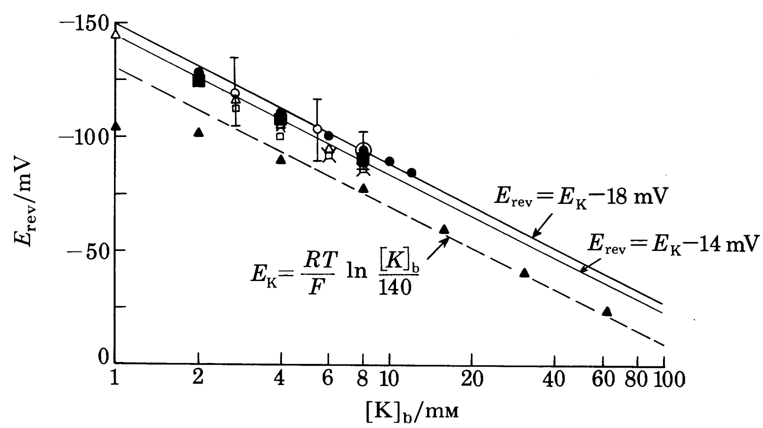

FIGURE 18. Variation of E_{rev} for 'i_{K2}' with $[K]_b$ given by the model and by various experimental results. We also show the results on measurements of resting potentials and the predictions of the Nernst equation for potassium (interrupted line) and of (66) (solid lines) for two values of ΔE. ● Model 1; ■ model 2; □ Noble & Tsien 1968; △ Peper & Trautwein 1969; ○ Cohen *et al.* 1976; × DiFrancesco *et al.* 1979*b*; ▲ resting potential (Gadsby & Cranefield 1977).

logarithmic scale. The filled square symbols show the results for the present model, while the filled round symbols show the results for the earlier version (DiFrancesco & Noble 1982). The open symbols show the results of various experiments, while the filled triangles show the variation in resting potential obtained by Gadsby & Cranefield (1977). The interrupted line shows the value for E_K computed by assuming that $[K]_i = 140$ mM. This is clearly a good fit to the resting potential results for values of $[K]_b$ above about 8 mM. Equally clearly, all the reversal potential estimates, experimental and theoretical lie significantly negative to the estimated values of E_K. To a first approximation, the results fit an equation of the form:

$$E_{rev} = E_K - \Delta E \tag{66}$$

where ΔE is nearly a constant. For the early version of the model the best value of ΔE is 18 mV. For the present version it lies at about 14 mV. The theoretical derivation of and justification for this surprisingly simple equation has been given already in DiFrancesco & Noble (1982). All we need to add to what was shown in that paper is that we have now checked this result with numerical computations in about eight different versions of the same basic model with various formulations of i_{K1} and i_f. Any lingering suspicion that the result is fortuitous can now be laid firmly to rest. Given the properties of i_{K1} and its strong K-dependence at negative potentials and the similar time constants for the y gating reaction and the K^+ depletion process an approximate equation of the form of (59) is far from fortuitous: it is rather a necessary consequence of the given properties of the ionic currents and geometries involved.

Nevertheless, there are some significant variations. First, as shown by the comparison between the two versions of our model, the best value for ΔE can vary. Among the variables concerned in determining this parameter is the size of the extracellular cleft space (DiFrancesco & Noble 1982). Secondly, it is worth noting that the precise shape of the ionic current record near the reversal potential varies with the detailed characteristics assumed. Sometimes the current record remains virtually monotonic (cf. Noble & Tsien 1968, figure 5, and the results plotted in figure 18). Sometimes, it is clearly biphasic (cf. Cohen *et al.* (1976), figure 2B, and the computed results shown in DiFrancesco & Noble (1980*c*)). It is even sometimes impossible to obtain a reversal potential (see, for example, Cohen *et al.* (1976), figure 2C). This is of course the natural situation in the mammalian s.a. node where i_{K1} is too weak to produce sufficient depletion dependent current change to mask i_f. It is therefore significant that the case showing absence of reversal published by Cohen *et al.* (1976) is from a Purkinje fibre in which the instantaneous current jumps attributable primarily to i_{K1} were very small indeed. It is easy to produce this behaviour in the model by reducing i_{K1} (DiFrancesco & Noble 1982).

Recently, Clay & Shrier (1981*a*, *b*) have recorded an ionic current change in spherical aggregates of embryonic ventricular cells which strongly resembles i_f or i_{K2}. In their analysis they use the Noble & Tsien (1968) i_{K2} hypothesis. We therefore thought it important to check the extent to which their results are also compatible with an i_f hypothesis. To reproduce their experimental situation we made the following modifications to the model: (i) the equations for K^+ diffusion in a spherical space were used instead of the cylindrical equations; (ii) the sphere was assumed to have a radius of 100 μm with an extracellular space volume of 4% (the values given by Clay & Shrier (1981*a*, *b*)); (iii) the ionic currents were all scaled down by a factor of 10 to give absolute values similar to those recorded in Clay & Shrier's experiments. We have in fact repeated the computations for a variety of other parameter sets (see, for example, DiFrancesco & Noble (1981) for an example that uses Clay & Shrier's kinetics). The results all resemble those shown in figure 19 which shows currents computed in response to

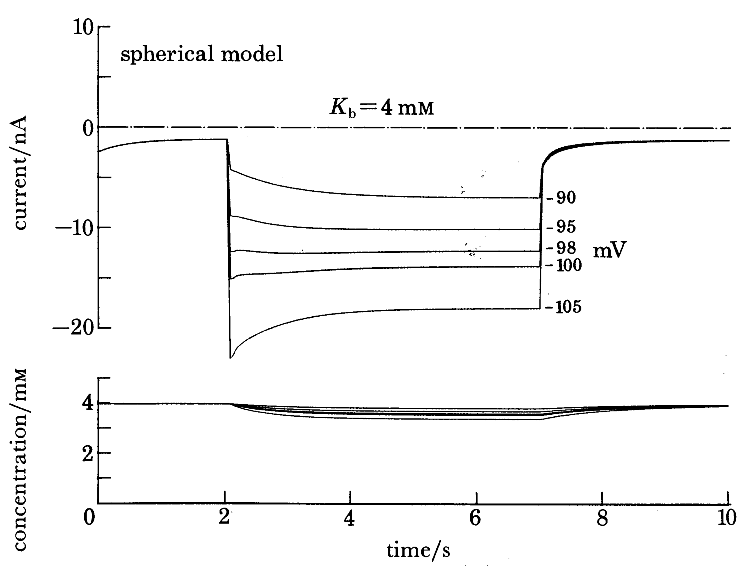

FIGURE 19. Computed variations in ionic current in a spherical model in response to various hyperpolarizations from −50 mV to the potentials shown. The extracellular cleft space was set to 4%. The full diffusion equations for a three-dimensional spherical space were used. The mean values of $[K]_c$ are plotted below. $[K]_i$ was set to 110 mM. This gives a reversal potential at −98 mV.

hyperpolarizations from -50 mV with the bulk [K] set at 4 mM. To obtain a 'reversal' potential at about -98 mV (near the value found by Clay & Shrier) we used a value of 110 mM for $[K]_i$. The results clearly closely resemble those of Clay & Shrier. A feature of their results which they feel strongly supports the i_{K2} hypothesis is that the current records at the reversal potential are very flat. The result computed in figure 19 shows only 2% variation in current level at the reversal potential. This figure depends naturally on the precise parameters assumed. With other possible parameters consistent with the experimental data, this figure for the current variation at E_{rev} could be higher or lower. Our own view is that this is not the crucial argument for distinguishing between the hypothesis. The more important one is to ask, first, what is the minimum plausible magnitude of the depletion process during hyperpolarization to E_{rev} and, second, would the change in i_{K1} expected from such a change in $[K]_c$ be within, say, less than 1 or 2% of the total current. The answer to the first question is already provided in figure 19. It should be noted that in our computations using the full diffusion equations (in this case for a three-dimensional spherical space) we have used the free diffusion coefficient either with no restriction factor, or with a restriction factor of 0.5 to represent possible slowing of diffusion in the extracellular space either by the cells or by the external matrix. The computations were very similar for both situations since only the K concentration very near the surface was found to depend strongly on the diffusion coefficient. For a 4% space this gives a mean depletion of about 0.5 mM at the reversal potential (in the region of -98 mV). Now in this range of potentials the observed variation of ionic current with external K^+ is very large: from Clay & Shrier (1981 *a*, figure 2) we estimate of the order of 5–7 nA mM^{-1}, or about 2.5–3.5 nA for 0.5 mM change in $[K]_c$. Clearly such a current change is much larger than 1–2% of the total current; it is more like 20–30%. On this argument, a truly flat current record at about -95 mV requires that some other process (such as a slow activation of an inward current) should also occur, rather than being evidence for a single component. Put another way, to reduce the predicted cleft K^+ depletion to values (say less than 0.025 mM) sufficiently small to produce a less than 1–2% variation in ionic current we would have to increase the cleft space volume by at least a factor of 10 to about 40–50%. This is far from the value given by Clay & Shrier and, we suspect, much larger than an extracellular space size could possibly be in a tight-fitting cell aggregate. Our conclusion here, therefore, is that it is quantitatively implausible to hold that depletion is negligible in a 100 μm radius sphere conducting strongly K^+-dependent ionic currents of the magnitudes recorded by Clay & Shrier.

Conclusions

We have discussed most of our results together with their presentation since it is not possible in a paper of this kind to defer all the discussion to a separate section. In this concluding section we shall therefore restrict ourselves to discussion of a more general nature.

In one sense, our model is conceived in a manner similar to previous ones. In other ways it is a radical departure from them. The sense in which it resembles previous cardiac models is that it uses the experimental data on individual ionic current mechanisms to construct a mathematical description that acts as a convenient quantitative catalogue of the relevant results. While being primarily descriptive, this function of a model is nevertheless important and its importance grows as the number of separate mechanisms increases. Cardiac electrophysiology has long ago passed the stage at which numerical predictions on the basis of known experimental data are sufficiently obvious not to require a proper overall formulation. Even from this point of view our model is a major advance on the previous ones, and on the M.N.T. model in particular, since we have taken the opportunity to incorporate a very large range of new experimental information. Moreover, even at this simply descriptive level, it has already proved very useful in, for example, exploring the consequences of the very much faster kinetics determined for the calcium channel for the role of this channel in the action potential plateau, in reassessing the variations in ionic conductances during the action potential and pacemaker potential, and in reconstructing the influence of extracellular potassium ions on electrical activity. Viewed simply as an up-dating of the numerical catalogue, the model clearly replaces the M.N.T. model for the kinds of purpose for which that model was constructed.

Nevertheless, up-dating the M.N.T. model was not our initial or even primary aim. This was, rather, to begin to construct a model that, for the first time, fully integrates the electrophysiological description of gated channels in the heart with a description of the ionic pump and sequestering processes. The present state of development of the field clearly requires a model of this kind since it is no longer plausible to ignore either the direct contributions of ionic pumps and exchange mechanisms or the indirect effects arising from ion concentration changes. Doubtless, these underlie the well-known fact that cardiac muscle electrical activity changes in quite complex ways with time, and over a time scale that must involve changes in intracellular and extracellular ion concentrations. In addition to the examples provided by the computations described in the present paper, good examples of uses of the model that exploit this integration are the complete 'mapping' of the old i_{K2} hypothesis onto the new i_f hypothesis which we described in a previous paper (DiFrancesco & Noble 1982) and the use by Hart *et al.* (1983) to account for the transient nature of some of the electrical correlates of perturbation of the Na–K pump by low concentrations of cardiotonic steroids. Further examples are also provided by the extensive use of the mammalian s.a. node version of the model (Noble & Noble 1984) to provide plausible explanations for a variety of otherwise puzzling results obtained recently in experiments on this tissue (Brown *et al.* 1984*a*, *b*). We shall give further examples in DiFrancesco *et al.* (1985) which relate to longer-term changes and to possible interrelations between inotropic state and electrical properties. This also is an area that no useful model of electrical activity could now properly ignore. Our own initial involvement in the need to take account of ionic concentration changes was of course due to the requirement to investigate the theoretical consequences of potassium depletion processes in the extracellular spaces; it is an obvious and logical step to extend this approach to intracellular spaces.

While it was relatively easy to carry out this extension in principle, we have found it difficult to make some of the choices we found were necessary. It is extremely unlikely that our representation of the Ca-sequestering processes or of the Na–Ca exchange mechanism or of other Ca-activated currents (such as i_{to}) will remain among the best available for very long. Yet, our own experience (like that of McAllister *et al.* (1975)) is that the development of an overall model for the heart is a tedious process requiring at least two or three years and indefinite amounts of computer time. It was largely for this reason that we decided to program the model in a high structured language (Algol) that readily allows future developments. Many of the possible future developments are already built-in to the program and, as noted in the Methods section, we have translated the program into the closely related language, Pascal. Our hope is that those who wish to build onto the structure we have created will be able to do so relatively easily.

Finally, some comments are appropriate on a few choices in the development of the model that we could have made but didn't. First of all, we were inclined at an early stage to conclude that it would be most economical to assume that all or a major part of the background Na current is carried by non-specific (as between Na and K ions) Ca-activated channels of the kind described recently by Colqhoun *et al.* (1981) in the heart and which have also been observed in a wide variety of other tissues. This facility exists in the program and we spent several months investigating its consequences. While it is perfectly possible to construct a Purkinje fibre model in which this assumption is made, the assumption created fairly severe difficulties in extending the model to other tissues such as the s.a. node (Noble & Noble 1984) and ventricle (DiFrancesco *et al.* 1985). The reason is fairly simple. In a tissue in which the plateau potential is near the reversal potential of the non-specific channel the channel carries little current even when strongly Ca-activated and so does not greatly influence the action potential shape. By contrast, in preparations with fairly positive plateau potentials, the channel would carry fairly substantial outward currents. The result is in all cases to deform the repolarization process so that it resembles the Purkinje fibre repolarization process. Niedergerke & Page (1982) have recently shown that incorporating this channel mechanism into the M.N.T. model or the Beeler–Reuter model produces just this effect and that this may explain the shape of frog action potentials in high calcium at higher frequencies. This kind of repolarization waveform may also accompany what is usually called the 'rested state' contraction. In both cases, the contraction, and therefore the $[Ca]_i$ transient, are very large. Our results would fully confirm Niedergerke & Page's conclusions, but clearly this process cannot be significantly involved in action potentials from nodal or ventricular tissue when they do not show this particular repolarization waveform. Our conclusion here is that the full role and significance of this channel remains to be clarified. It may well be activated during unusually large $[Ca]_i$ transients, but it cannot be significantly activated during normal ventricular action potentials of the type in which the net repolarizing current is at its minimum during the $[Ca]_i$ transient.

Another area in which we initially explored some unsatisfactory formulations is the description of the Na–Ca exchange process. While there is now little doubt that this process is electrogenic, there are many ways in which its dependence on ionic concentrations and membrane potential might be formulated. We have satisfied ourselves that the simple hyperbolic sine function (see Mullins (1981), p. 42) is unsatisfactory except for a very restricted range of purposes when the only significant variable is membrane potential. In practice this is hardly ever the case since calcium concentration changes are nearly always involved. At the least, therefore, a better description of the Ca-dependence of the current is required. Yet, a complete version (whether that of Mullins (1977) or any other plausible model) of the equations for Na–Ca exchange would be so complex and use so many arbitrary coefficients that it would be cumbersome to formulate and would be of doubtful validity. We eventually opted for a compromise: a version that does incorporate a plausible description of the Ca-dependence of the exchange process but which does not fully represent the Na-dependence. This was achieved by representing a number of the Na-dependent terms in Mullins' model by a constant. We draw attention to this so as to warn other users of the model that, if substantial changes in Na concentrations are involved and the Na–Ca current is very significant, then they may have to develop the equations further than we have done in this direction. The possible roles of the Na–Ca exchange current have been quite extensively discussed recently. Our model may allow some of the questions raised to be put to some quantitative tests.

We should like to acknowledge the support of the Medical Research Council and of the British Heart Foundation. We are particularly grateful to the Wellcome Trust for providing support for Dr D. DiFrancesco, and to the Medical Research Council for the award of a Research Fellowship for Academic Staff to Dr D. Noble.

We should like to thank Dr F. Edwards for his invaluable help in setting up the PDP computer systems we used. We are also grateful to Dr G. Hart, Dr H. F. Brown, Dr K. S. Lee, Dr S. J. Noble, Dr T. Powell and Dr A. Taupignon for their comments on the manuscript of this paper.

References

Allen, D. G. & Kurihara, S. 1980 Calcium transients in mammalian ventricular muscle. *Eur. Heart J.* **1**, 5–15.

Attwell, D. & Cohen, I. 1977 The voltage clamp of multicellular preparations. *Prog. Biophys. molec. Biol.* **31**, 201–245.

Attwell, D., Cohen, I., Eisner, D., Ohba, M. & Ojeda, C. 1979*a* The steady-state TTX sensitive ('window') sodium current in cardiac Purkinje fibres. *Pflügers Arch. Eur. J. Physiol.* **379**, 137–142.

Attwell, D., Eisner, D. A. & Cohen, I. 1979*b* Voltage clamp and tracer flux data: effects of a restricted extracellular space. *Q. Rev. Biophys.* **12**, 213–261.

Attwell, D. & Jack, J. J. B. 1978 The interpretation of current–voltage relations: a Nernst–Planck analysis. *Prog. Biophys. molec. Biol.* **34**, 81–107.

Beeler, G. W. & McGuigan, J. A. S. 1978 Voltage clamping of multicellular myocardial preparations: capabilities and limitations of existing methods. *Prog. Biophys. molec. Biol.* **34**, 219–254.

Beeler, G. W. & Reuter, H. 1970*a* Membrane calcium current in ventricular myocardial fibres. *J. Physiol., Lond.* **207**, 165–190.

Beeler, G. W. & Reuter, H. 1970*b* The relation between membrane potential, membrane currents and activation of contraction in ventricular myocardial fibres. *J. Physiol., Lond.* **297**, 211–229.

Beeler, G. W. & Reuter, H. 1977 Reconstruction of the action potential of ventricular myocardial fibres. *J. Physiol., Lond.* **268**, 177–210.

Boyett, M. R. 1981*a* A study of the effect of the rate of stimulation on the transient outward current in sheep cardiac Purkinje fibres. *J. Physiol., Lond.* **139**, 1–22.

Boyett, M. R. 1981*b* Two transient outward currents in cardiac Purkinje fibres. *J. Physiol., Lond.* **320**, 32*P*.

Boyett, M. R. & Jewell, B. R. 1980 Analysis of the effects of changes in rate and rhythm upon electrical activity in the heart. *Prog. Biophys. molec. Biol.* **36**, 1–52.

Brown, A. M., Lee, K. S. & Powell, T. 1981 Sodium in single rate heart muscle cells. *J. Physiol., Lond.* **318**, 479–500.

Brown, H. F., Clark, A. & Noble, S. J. 1972 Analysis of pacemaker and repolarization currents in frog atrial muscle. *J. Physiol., Lond.* **258**, 547–577.

Brown, H. F., DiFrancesco, D., Noble, D. & Noble, S. J. 1980 The contribution of potassium accumulation to outward current in frog atrium. *J. Physiol., Lond.* **306**, 127–149.

Brown, H. F., Kimura, J., Noble, D., Noble, S. J. & Taupignon, A. 1983 Two components of 'second inward current' in the rabbit SA node. *J. Physiol., Lond.* **334**, 56*P*.

Brown, H. F., Kimura, J., Noble, D., Noble, S. J. & Taupignon, A. 1984*a* The slow inward current, i_{si}, in the rabbit sino-atrial node investigated by voltage clamp and computer simulation. *Proc. R. Soc. Lond.* B **222**, 305–328.

Brown, H. F., Kimura, J., Noble, D., Noble, S. J. & Taupignon, A. 1984*b* The ionic currents underlying pacemaker activity in rabbit sino-atrial node: experimental results and computer simulation. *Proc. R. Soc. Lond.* B **222**, 329–347.

Carmeliet, E. 1980 Decrease of K efflux and influx by external Cs ions in cardiac Purkinje and muscle cells. *Pflügers Arch. Eur. J. Physiol.* **383**, 143–150.

Carmeliet, E. 1982 Induction and removal of inward-going rectification in sheep cardiac Purkinje fibres *J. Physiol., Lond.* **327**, 285–308.

Chandler, W. K. & Meves, H. 1965 Voltage clamp experiments on internally perfused giant axons. *J. Physiol., Lond.* **180**, 821–836.

Chapman, R. A. 1979 Excitation-contraction coupling in cardiac muscle. *Prog. Biophys. molec. Biol.* **35**, 1–52.

Chapman, R. A., Coray, A. & McGuigan, J. A. S. 1983 Sodium/calcium exchange in mammalian ventricular muscle: a study with sodium-sensitive microelectrodes. *J. Physiol., Lond.* **343**, 253–276.

Chapman, R. A. & Tunstall, J. 1980 The interaction of sodium and calcium ions at the cell membrane and the control of contractile strength in frog atrial muscle. *J. Physiol., Lond.* **305**, 109–123.

Clay, J. R. & Shrier, A. 1981*a* Analysis of subthreshold pacemaker currents in chick embryonic heart cells. *J. Physiol., Lond.* **312**, 471–490.

Clay, J. R. & Shrier, A. 1981*b* Developmental changes in subthreshold pace-maker currents in chick embryonic heart cells. *J. Physiol., Lond.* **312**, 491–504.

Clusin, W. T., Fischmeister, R. & deHaan, R. L. 1983 Caffeine-induced current in embryonic heart cells: time course and voltage dependence. *Am. J. Physiol.* **254**, H528–H532.

Cohen, I., Daut, J. & Noble, D. 1976 The effects of potassium and temperature on the pacemaker current i_{K2} in Purkinje fibres. *J. Physiol., Lond.* **260**, 55–74.

Cohen, I., Eisner, D. A. & Noble, D. 1978 The action of adrenaline on pacemaker activity in cardiac Purkinje fibres. *J. Physiol., Lond.* **280**, 155–168.

Cohen, I. S., Falk, R. T. & Mulrine, N. K. 1983 Actions of barium and rubidium on membrane currents in canine Purkinje fibres. *J. Physiol., Lond.* **338**, 589–612.

Colatsky, T. J. 1980 Voltage clamp measurements of sodium channel properties in rabbit cardiac Purkinje fibres. *J. Physiol., Lond.* **305**, 215–234.

Colatsky, T. J. 1982 Mechanisms of action of lidocaine and quinidine on action potential duration in rabbit cardiac Purkinje fibres. *Circ. Res.* **50**, 17–27.

Colatsky, T. J. & Gadsby, D. C. 1980 Is tetrodotoxin block of background sodium channels in canine Purkinje fibres voltage-dependent? *J. Physiol., Lond.* **306**, 20*P*.

Colatsky, T. J. & Tsien, R. W. 1979 Electrical properties associated with wide intercellular clefts in rabbit Purkinje fibres. *J. Physiol., Lond.* **290**, 227–252.

Colquhoun, D., Neher, E., Reuter, H. & Stevens, C. F. 1981 Inward channels activated by intracellular Ca in cultured heart cells. *Nature, Lond.* **294**, 752–754.

Coraboeuf, E. & Carmeliet, E. 1982 Existence of two transient outward channels in sheep cardiac Purkinje fibres. *Pflügers Arch. Eur. J. Physiol.* **392**, 352–359.

Coraboeuf, E. & Deroubaix, E. 1978 Shortening effect of tetrodotoxin on action potentials of the conducting system in the dog heart. *J. Physiol., Lond.* **280**, 24*P*.

Coraboeuf, E., Gautier, P. & Guiraudou, P. 1981 Potential and tension changes induced by sodium removal in dog Purkinje fibres: role of an electrogenic sodium–calcium exchange. *J. Physiol., Lond.* **311**, 605–622.

Deitmer, J. W. & Ellis, D. 1978 The intracellular sodium activity of cardiac Purkinje fibres during inhibition and reactivation of the sodium–potassium pump. *J. Physiol., Lond.* **284**, 241–259.

DiFrancesco, D. 1981*a* A new interpretation of the pace-maker current i_{K2} in Purkinje fibres. *J. Physiol., Lond.* **314**, 359–376.

DiFrancesco, D. 1981*b* A study of the ionic nature of the pace-maker current in calf Purkinje fibres. *J. Physiol., Lond.* **314**, 377–393.

DiFrancesco, D. 1982 Block and activation of the pace-maker channel in calf Purkinje fibres: effects of potassium, caesium and rubidium. *J. Physiol., Lond.* **329**, 485–507.

DiFrancesco, D. 1984 Characterization of the pacemaker (i_f) current kinetics in calf Purkinje fibres. *J. Physiol., Lond.* **348**, 341–367.

DiFrancesco, D. & Ferroni, A. 1983 Delayed activation of the cardiac pacemaker current and its dependence on conditioning pre-hyperpolarizations. *Pflügers Arch. Eur. J. Physiol.* **396**, 265–267.

DiFrancesco, D., Hart, G. & Noble, D. 1982 Ionic current transients attributable to the Na–Ca exchange process in the heart: computer model. *J. Physiol., Lond.* **328**, 15*P*.

DiFrancesco, D., Hart, G. & Noble, D. 1983 Demonstration of oscillatory variations in $[Ca]_i$ and membrane currents in a computer model of Ca-induced Ca release in mammalian Purkinje fibre and ventricular muscle. *J. Physiol., Lond.* **334**, 8*P*.

DiFrancesco, D., Hart, G. & Noble, D. 1985 (In preparation.)

DiFrancesco, D. & McNaughton, P. A. 1979 The effects of calcium on outward membrane currents in the cardiac Purkinje fibre. *J. Physiol., Lond.* **289**, 347–373.

DiFrancesco, D. & Noble, D. 1980*a* The time course of potassium current following potassium accumulation in frog atrium: analytical solutions using a linear approximation. *J. Physiol., Lond.* **306**, 152–173.

DiFrancesco, D. & Noble, D. 1980*b* Reconstruction of Purkinje fibre currents in sodium-free solution. *J. Physiol., Lond.* **308**, 35*P*.

DiFrancesco, D. & Noble, D. 1980*c* If 'i_{K2}' is an inward current, how does it display potassium specificity? *J. Physiol., Lond.* **305**, 14.

DiFrancesco, D. & Noble, D. 1981 A model of cardiac electrical activity incorporating restricted extracellular spaces and the sodium potassium pump. *J. Physiol., Lond.* **320**, 25*P*.

DiFrancesco, D. & Noble, D. 1982 Implications of the re-interpretation of i_{K2} for the modelling of the electrical activity of pacemaker tissues in the heart. In *Cardiac rate and rhythm* (ed. L. N. Bouman and H. J. Jongsma), pp. 93–128. The Hague: Martinus Nijhoff.

DiFrancesco, D., Noma, A. & Trautwein, W. 1979*a* Kinetics and magnitude of the time-dependent K current in the rabbit SA node: effect of external potassium. *Pflügers Arch. Eur. J. Physiol.* **381**, 271–279.

DiFrancesco, D., Ohba, M. & Ojeda, C. 1979*b* Measurement and significance of the reversal potential for the pacemaker current i_{K2} in sheep Purkinje fibres. *J. Physiol., Lond.* **297**, 135–162.

Draper, M. H. & Weidmann, S. 1951 Cardiac resting and action potentials recorded with an intracellular electrode. *J. Physiol., Lond.* **115**, 74–94.

Dudel, J., Peper, K., Rüdel, R. & Trautwein, W. 1967*a* The dynamic chloride component of membrane current in Purkinje fibres. *Pflügers Arch. Eur. J. Physiol.* **295**, 197–212.

Dudel, J., Peper, K., Rüdel, R. & Trautwein, W. 1967*b* The potassium component of membrane current in Purkinje fibres. *Pflügers Arch. Eur. J. Physiol.* **296**, 308–327.

Ebihara, L., Shigeto, N., Lieberman, M. & Johnson, E. A. 1980 The initial inward current in spherical clusters of chick embryonic heart cells. *J. gen. Physiol.* **75**, 437–456.

Eisner, D. A. & Lederer, W. J. 1980 Characterization of the sodium pump in cardiac Purkinje fibres. *J. Physiol., Lond.* **303**, 441–474.

Eisner, D. A., Lederer, W. J. & Noble, D. 1979 Caffeine and tetracaine abolish the slow inward current in sheep cardiac Purkinje fibres. *J. Physiol., Lond.* **293**, 76*P*.

Eisner, D. A., Lederer, W. J. & Vaughan-Jones, R. 1981 The dependence of sodium pumping and tension on intracellular sodium activity in voltage-clamped sheep Purkinje fibres. *J. Physiol., Lond.* **317**, 167–187.

Ellis, D. 1977 The effects of external cations and ouabain on the intracellular sodium activity of sheep heart Purkinje fibres. *J. Physiol., Lond.* **274**, 211–240.

Fabiato, A. & Fabiato, F. 1975 Contractions induced by a calcium-triggered release of calcium from the sarcoplasmic reticulum of single skinned cardiac cells. *J. Physiol., Lond.* **249**, 469–495.

Fischmeister, R. & Vassort, G. 1981 The electrogenic Na/Ca exchange and the cardiac electrical activity. 1. Simulation on Purkinje fibre action potential. *J. Physiol., Paris* **77**, 705–709.

Fozzard, H. & Hiraoka, M. 1973 The positive dynamic current and its inactivation properties in cardiac Purkinje fibres. *J. Physiol., Lond.* **234**, 569–586.

Gadsby, D. C. 1980 Activation of electrogenic Na^+/K^+ exchange by extracellular K^+ in canine cardiac Purkinje fibres. *Proc. natn. Acad. Sci. U.S.A.* **77**, 4035–4039.

Gadsby, D. C. 1982 Hyperpolarization of frog skeletal muscle fibres and canine cardiac Purkinje fibres during enhanced K^+–Na^+ exchange: extracellular K^+ depletion or increased pump current? *Curr. Top. Memb. Transport.* **16**, 17–34.

Gadsby, D. C. & Cranefield, P. F. 1977 Two levels of resting potential in cardiac Purkinje fibers. *J. gen. Physiol.* **70**, 725–746.

Gadsby, D. C. & Cranefield, P. F. 1979 Electrogenic sodium extrusion in cardiac Purkinje fibers. *J. gen. Physiol.* **73**, 819–837.

Gibbons, W. R. & Fozzard, H. A. 1975*a* Relationships between voltage and tension in sheep cardiac Purkinje fibers. *J. gen. Physiol.* **65**, 345–365.

Gibbons, W. R. & Fozzard, H. A. 1975*b* Slow inward current and contraction of sheep cardiac Purkinje fibers. *J. gen. Physiol.* **65**, 367–384.

Gintant, G. A., Datyuner, N. B. & Cohen, I. 1984 Slow inactivation of a tetrodotoxin-sensitive current in canine cardiac Purkinje fibres. *Biophys. J.* (In the press.)

Haas, H. G. & Kern, R. 1966 Potassium fluxes in voltage clamped Purkinje fibres. *Pflügers Arch. Eur. J. Physiol.* **291**, 69–84.

Hagiwara, S. & Takahashi, K. 1974 The anomalous rectification and cation selectivity of the membrane of a starfish egg cell. *J. membrane Biol.* **18**, 61–80.

Hall, A. E., Hutter, O. F. & Noble, D. 1963 Current–voltage relations of Purkinje fibres in sodium-deficient solutions. *J. Physiol., Lond.* **166**, 225–240.

Hart, G. 1983 The kinetics and temperature dependence of the pacemaker current i_f in sheep Purkinje fibres. *J. Physiol., Lond.* **337**, 401–416.

Hart, G., Noble, D. & Shimoni, Y. 1980 Adrenaline shifts the voltage dependence of the sodium and potassium components of i_f in sheep Purkinje fibres. *J. Physiol., Lond.* **308**, 34*P*.

Hart, G., Noble, D. & Shimoni, Y. 1982 Analysis of the early outward currents in sheep Purkinje fibres. *J. Physiol., Lond.* **326**, 68*P*.

Hart, G., Noble, D. & Shimoni, Y. 1983 The effects of low concentrations of cardiotonic steroids on membrane currents and tension in sheep Purkinje fibres. *J. Physiol., Lond.* **334**, 103–131.

Hauswirth, O., Noble, D. & Tsien, R. W. 1968 Adrenaline: mechanism of action on the pacemaker potential in cardiac Purkinje fibres. *Science, Wash.* **162**, 916–917.

Hauswirth, O., Noble, D. & Tsien, R. W. 1969 The mechanism of oscillatory activity at low membrane potentials in cardiac Purkinje fibres. *J. Physiol., Lond.* **200**, 255–265.

Hauswirth, O., Noble, D. & Tsien, R. W. 1972 The dependence of plateau currents in cardiac Purkinje fibres on the interval between action potentials. *J. Physiol., Lond.* **222**, 27–49.

Hille, B. & Schwartz, W. 1978 Potassium channels as multi-ion single-file pores. *J. gen. Physiol.* **72**, 409–442.

Hodgkin, A. L. & Horowitz, P. 1960 Potassium contractures in single muscle fibres. *J. Physiol., Lond.* **153**, 386–403.

Hodgkin, A. L. & Huxley, A. F. 1952 A quantitative description of membrane current and its application to conduction and excitation in nerve. *J. Physiol., Lond.* **117**, 500–544.

Hodgkin, A. L. & Katz, B. 1949 The effect of sodium ions on the electrical activity of the giant axon of the squid. *J. Physiol., Lond.* **108**, 37–77.

Horackova, M. & Vassort, G. 1979 Sodium–calcium exchange in regulation of cardiac contractility. Evidence for an electrogenic voltage-dependent mechanism. *J. gen. Physiol.* **73**, 403–424.

Hume, J. R. & Giles, W. R. 1983 Ionic currents in single isolated bullfrog atrial cells. *J. gen. Physiol.* **81**, 153–194.

Isenberg, G. 1976 Cardiac Purkinje fibres: caesium as a tool to block inward rectifying potassium currents. *Pflügers Arch. Eur. J. Physiol.* **365**, 99–106.

Isenberg, G. & Klöckner, V. 1982 Calcium currents of isolated bovine ventricular myocytes are fast and of large amplitude. *Pflügers Arch. Eur. J. Physiol.* **195**, 30–41.

Isenberg, G. & Trautwein, W. 1974 The effect of dihydroouabain and lithium ions on the outward current in cardiac Purkinje fibres. Evidence for electrogenicity of active transport. *Pflügers Arch. Eur. J. Physiol.* **350**, 41–54.

Jack, J. J. B., Noble, D. & Tsien, R. W. 1975 *Electric current flow in excitable cells.* Oxford: Clarendon Press. (Paperback edition, 1983.)

Johnson, E. A. & Lieberman, M. 1971 Heart: excitation and contraction. *A. Rev. Physiol.* **33**, 499–532.

Kass, R. S. & Wiegers, S. E. 1982 The ionic basis of concentration related effects of noradrenaline on the action potential of calf cardiac Purkinje fibres. *J. Physiol., Lond.* **322**, 541–558.

Kenyon, J. L. & Gibbons, W. R. 1979 4-aminopyridine and the early outward current of sheep cardiac Purkinje fibres. *J. gen. Physiol.* **73**, 139–157.

Lederer, W. J. & Eisner, D. A. 1982 The effects of sodium pump activity on the slow inward current in sheep cardiac Purkinje fibres. *Proc. R. Soc. Lond.* B **214**, 249–262.

Lee & Fozzard, H. A. 1975 Activities of potassium and sodium ions in rabbit heart muscle. *J. gen. Physiol.* **65**, 695–708.

Lee, E., Lee, K. S., Noble, D. & Spindler, A. J. 1983 A very slow inward current in single ventricular cells. *J. Physiol., Lond.* **345**, 6*P*.

Lee, E., Lee, K. S., Noble, D. & Spindler, A. J. 1984*a* A new, very slow inward Ca current in single ventricular cells of adult guinea-pig. *J. Physiol., Lond.* **346**, 75*P*.

Lee, E., Lee, K. S., Noble, D. & Spindler, A. J. 1984*b* Further properties of the very slow inward currents in isolated single guinea-pig cells. *J. Physiol., Lond.* (In the press.)

Lee, K. S. & Tsien, R. W. 1982 Reversal of current through calcium channels in dialyzed heart cells. *Nature, Lond.* **297**, 498–501.

Lee, K. S., Weeks, T. A., Kao, R. L., Akaike, N. & Brown, A. M. 1979 Sodium current in single heart muscle cells. *Nature, Lond.* **278**, 269–271.

McAllister, R. E. & Noble, D. 1966 The time and voltage dependence of the slow outward current in cardiac Purkinje fibres. *J. Physiol., Lond.* **186**, 632–662.

McAllister, R. E., Noble, D. & Tsien, R. W. 1975 Reconstruction of the electrical activity of cardiac Purkinje fibres. *J. Physiol., Lond.* **251**, 1–59.

McDonald, T. F. & Trautwein, W. 1978 The potassium current underlying delayed rectification in cat ventricular muscle. *J. Physiol., Lond.* **274**, 217–246.

Marban, E., Rink, T. J., Tsien, R. W. & Tsien, R. Y. 1980 Free calcium in heart muscle at rest and during contraction measured with Ca^{++}-sensitive microelectrodes. *Nature, Lond.* **286**, 845–850.

Mentrard, D. & Vassort, G. 1982 The Na–Ca exchange generates a current in frog heart cells. *J. Physiol., Lond.* **334**, 55*P*.

Mitchell, M. R., Powell, T., Sturridge, M. F., Terrar, D. A. & Twist, V. W. 1982 Action potentials and second inward current recorded from individual human ventricular muscle cells. *J. Physiol., Lond.* **332**, 51*P*.

Mitchell, M. R., Powell, T., Terrar, D. A. & Twist, V. W. 1983 Characteristics of the second inward current in cells isolated from rat ventricular muscle. *Proc. R. Soc. Lond.* B **219**, 447–469.

Miura, D. S., Hoffman, B. F. & Rosen, M. R. 1977 The effect of extracellular potassium on the intracellular potassium ion activity and transmembrane potentials of beating canine cardiac Purkinje fibres. *J. gen. Physiol.* **69**, 463–474.

Mobley, B. A. & Page, E. 1972 The surface area of sheep cardiac Purkinje fibres. *J. Physiol., Lond.* **220**, 547–563.

Modern computing methods 1961 London: Her Majesty's Stationery Office.

Momose, Y., Szabo, G. & Giles, W. R. 1983 An inwardly rectifying K^+ current in bullfrog atrial cells. *Biophys. J.* **41**, 311a.

Mullins, L. J. 1977 A mechanism for Na/Ca transport. *J. gen. Physiol.* **70**, 681–695.

Mullins, L. J. 1981 *Ion transport in the heart.* New York: Raven Press.

Niedergerke, R. 1963 Movements of Ca in beating ventricles of the frog. *J. Physiol., Lond.* **167**, 551–580.

Niedergerke, R. & Page, S. 1982 Changes of frog heart action potential due to intracellular calcium ions. *J. Physiol., Lond.* **328**, 17–18*P*.

Noble, D. 1962 A modification of the Hodgkin–Huxley equations applicable to Purkinje fibre action and pacemaker potentials. *J. Physiol., Lond.* **160**, 317–352.

Noble, D. 1965 Electrical properties of cardiac muscle attributable to inward-going (anomalous) rectification. *J. cell. comp. Physiol.* **66**, 127–136.

Noble, D. 1972 Conductance mechanisms in excitable cells. In *Biomembranes* 3 (ed. F. Kreuzer and J. F. G. Slegers), pp. 427–447. New York: Plenum Press.

Noble, D. 1979 *The initiation of the heartbeat.* 2nd edn. Oxford University Press.

Noble, D. 1984 The surprising heart: A review of recent progress in cardiac electrophysiology. *J. Physiol., Lond.* (In the press.)

Noble, D. & Noble, S. 1984 A model of sino-atrial node electrical activity based on a modification of the DiFrancesco–Noble (1984) equations. *Proc. R. Soc. Lond.* B **222**, 295–304.

Noble, D. & Tsien, R. W. 1968 The kinetics and rectifier properties of the slow potassium current in cardiac Purkinje fibres. *J. Physiol., Lond.* **195**, 185–214.

Noble, D. & Tsien, R. W. 1969*a* Outward membrane currents activated in the plateau range of potentials in cardiac Purkinje fibres. *J. Physiol., Lond.* **200**, 205–231.

Noble, D. & Tsien, R. W. 1969*b* Reconstruction of the repolarization process in cardiac Purkinje fibres based on voltage clamp measurements of the membrane current. *J. Physiol., Lond.* **200**, 233–254.

Plant, R. E. 1979 The efficient numerical solution of biological simulation problems. *Computer Progr. in Biomed.* **10**, 1–15.

Peper, K. & Trautwein, W. 1969 A note on the pacemaker current in Purkinje fibres. *Pflügers Arch. Eur. J. Physiol.* **309**, 356–361.

Powell, T., Terrar, D. A. & Twist, V. W. 1981 The effect of noradrenaline on slow inward current in rat ventricular myocytes. *J. Physiol., Lond.* **319**, 82*P*.

Reuter, H. 1967 The dependence of slow inward current in Purkinje fibres on the extracellular calcium concentration. *J. Physiol., Lond.* **192**, 479–492.

Reuter, H. & Scholz, H. 1977 A study on the ion selectivity and the kinetic properties of the calcium dependent slow inward current in mammalian cardiac muscle. *J. Physiol., Lond.* **264**, 17–47.

Reuter, H., Stevens, C. F., Tsien, R. W. & Yellen, G. 1982 Properties of single calcium channels in cardiac cell culture. *Nature, Lond.* **297**, 501–504.

Rougier, O., Vassort, G., Garnier, D., Gargouil, Y.-M. & Coraboeuf, E. 1969 Existence and rôle of a slow inward current during the frog atrial action potential. *Pflügers Arch. Eur. J. Physiol.* **308**, 91–110.

Sakmann, B. & Trube, G. 1984 Conductance properties of single inwardly rectifying potassium channels in ventricular cells from guinea-pig heart. *J. Physiol., Lond.* (In the press.)

Sheu, S. S. & Fozzard, H. A. 1982 Transmembrane Na^+ and Ca^{2+} electrochemical gradients in cardiac muscle and their relationship to force development. *J. gen. Physiol.* **80**, 325–351.

Siegelbaum, S. A. & Tsien, R. W. 1980 Calcium-activated transient outward current in calf cardiac Purkinje fibres. *J. Physiol., Lond.* **299**, 485–506.

Siegelbaum, S., Tsien, R. W. & Kass, R. S. 1977 Role of intracellular calcium in the transient outward current in calf Purkinje fibres. *Nature, Lond.* **269**, 611–613.

Sjodin, R. A. 1980 Contribution of Na/Ca transport to the resting membrane potential. *J. gen. Physiol.* **76**, 99–108.

Standen, N. B. & Stanfield, P. R. 1982 A binding site model for calcium channel inactivation that depends on calcium entry. *Proc. R. Soc. Lond.* B **217**, 101–110.

Tsien, R. W. 1974 Effects of epinephrine on the pacemaker potassium current of cardiac Purkinje fibres. *J. gen. Physiol.* **64**, 293–319.

Vasalle, M. 1966 Cardiac pacemaker potentials at different extra- and intracellular K concentrations. *Am. J. Physiol.* **208**, 770–775.

Vassalle, M. 1966 Analysis of cardiac pacemaker potentials using a 'voltage-clamp' technique. *Am. J. Physiol.* **210**, 1335–1341.

Vereecke, J., Isenberg, G. & Carmeliet, E. 1980 K efflux through inward rectifying K channels in voltage clamped Purkinje fibres. *Pflügers Arch. Eur. J. Physiol.* **384**, 207–217.

Weidmann, S. 1951 Effect of current flow on the membrane potential of cardiac muscle. *J. Physiol., Lond.* **115**, 227–236.

Weidmann, S. 1952 The electrical constants of Purkinje fibres. *J. Physiol., Lond.* **118**, 348–360.

Weidmann, S. 1956 *Elektrophysiologie der Herzmuskelfaser*. Bern: Huber.

Wier, W. G. 1980 Calcium transients during excitation-contraction coupling in mammalian heart: aequorin signals of canine Purkinje fibres. *Science, Wash.* **207**, 1085–1087.

Wier, W. G. & Isenberg, G. 1982 Intracellular [Ca] transients in voltage-clamped cardiac Purkinje fibres. *Pflügers Arch. Eur. J. Physiol.* **392**, 284–290.